# Results

3.1 Interaction between associative nitrogen-fixing bacteria and rice plant.

3.1.1 Attachment. *Klebsiella spp.* R15 or R17 (10^8 cells in 100 µl PBS) were inoculated in a culture tube containing 3 rice seedlings (7-day-old). Either equal number of *E. coli* or merely PBS buffer were added into the control tubes. Control samples without bacterial inoculation of PBS washed rice roots, and those inoculated with acridine orange labelled *E. coli* are devoid of attached bacteria (Fig. 2A and B) all through the observation period of 2-48 h. Adherence of live and fluorescent R15 and R17 on the root hairs and epidermal cells can be observed after 2 h of inoculation as loose cluster (Fig. 2C - F). Formation of numerous microcolony or bag-like structure enclosing live bacteria can be observed after 36 h of bacterial inoculation. The micronodule or bag-like structures entrapping R15 or R17 are typically spherical in shape (Fig. 2G - J). Scanning electron micrographs of control

Figure 2   Epi-fluorescence micrographs of rice (cv.RD7) seedling root with attached *Klebsiella spp.* R15 and R17.

Bacterial inoculum of 10^8 cells in 100 μl were added into 5 ml hydroponic culture of 3 rice seedlings. (Magnification x 450)

A, B   No attachment due to *E.coli* inoculation during 2 - 36 h.

C, D   Attachment as loose cluster of R15 on epidermal cells and root hairs at 2 h after inoculation.

E, F   Attachment as loose cluster of R17 on epidermal cells and root hairs at 2 h after inoculation.

G, H   Micronodule formation of R15 on root hairs and epidermal cells at 36 h after inoculation.

I, J   Micronodule formation of R17 on epidermal cells and root hairs at 36 h after inoculation.
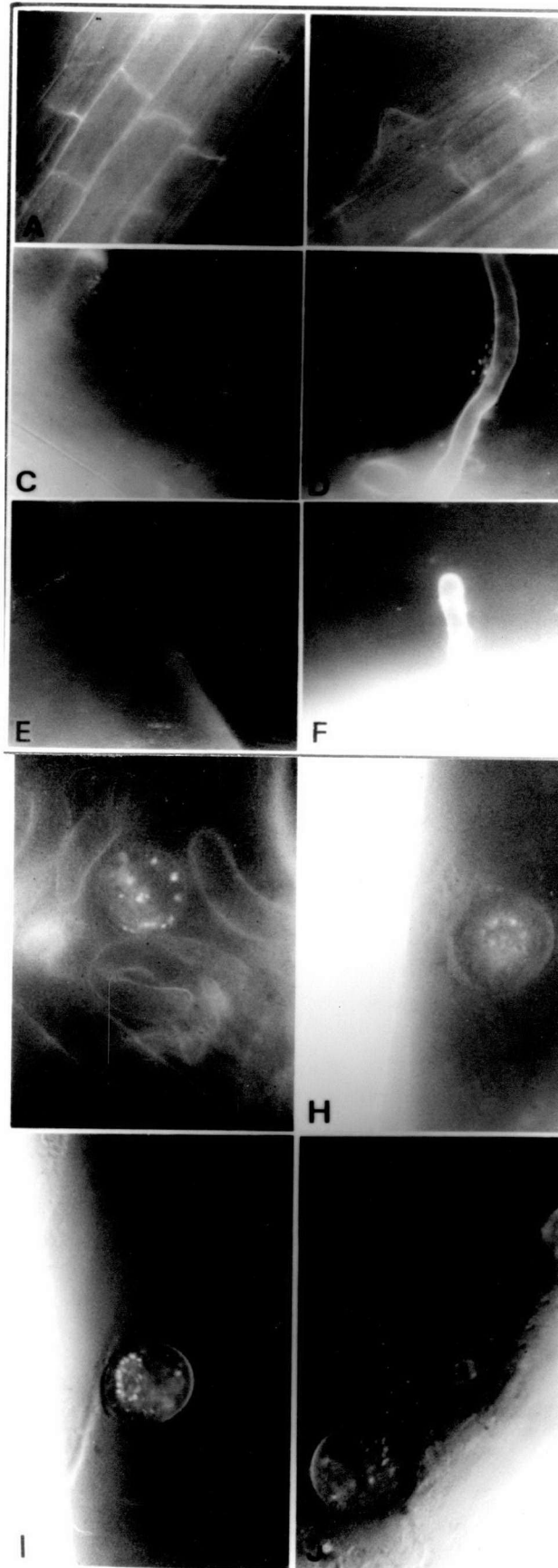
root samples inoculated with *E. coli* show little interaction of *E. coli* with rice roots (Fig. 3A - C) and do confirm numerous attachment of R15 and R17 on the root surface as single cells and loose agglutinated form at 2h after inoculation (Fig. 3D - G), and formation of spherical micronodule structures of the diameter about 10-15 μ at 36 h after inoculation (Fig. 3H - N). Reduction of inoculum size to 10^6 cells in 100 μl PBS of either R15 or R17 resulted in merely disperse attachment and loose cluster at 2 h up to 48 h after inoculation. No formation of micronodules can be observed (picture not shown) from both epi-fluorescence microscope and SEM.

3.1.2 Deformation and branching of root hairs. The scanning electron micrographs of control root samples inoculated with *E. coli* show normal feature of root hairs as observed in non-inoculated plants(Fig.3A-C), whereas deformation and branching of root hairs are obvious in root samples inoculated with either R15 or R17 (Fig. 3H - J and L - M).

3.1.3 Ultrastructure of micronodules. The root samples bearing micronodules were freeze-fractured at random and observed in a scanning electron microscope. Fig. 4 demonstrates the cross-section of rice root

Figure 3   Scanning electron micrographs of rice (cv.RD7) seedling root with attached *Klebsiella spp.* R15 and R17. Bacterial inoculum of 10^8 cells in 100 µl were added into 5 ml hydroponic culture of 3 rice seedlings.

A, B, C   Little interactition due to *E.coli* inoculation during 2-36 h.

D   Attachment as single cells of R15 on root epidermal cells at 2 h after inoculation.

E   Attachment as cluster of R15 on root epidermal cells at 16 h after inoculation.

F   Attachment as single cells of R17 on a root hair at 2 h after inoculation.

G   Attachment as cluster of R17 on root epidermal cells at 16 h after inoculation.

H, I, J   Micronodule formation of R15 on root hairs and epidermal cells, and deformation and branching of root hair, at 36 h after inoculation.

K   Micronodule of R15, spherical in shape with diameter about 10 µ at 36 h after inoculation.

L   Deformation and branching of root hairs, at 36 h after inoculation of R17.

M   Micronodule formation of R17 on a root hair at 36 h after inculation.

N   Micronodule of R17, spherical in shape with diameter about 10 µ at 36 h after inoculation.
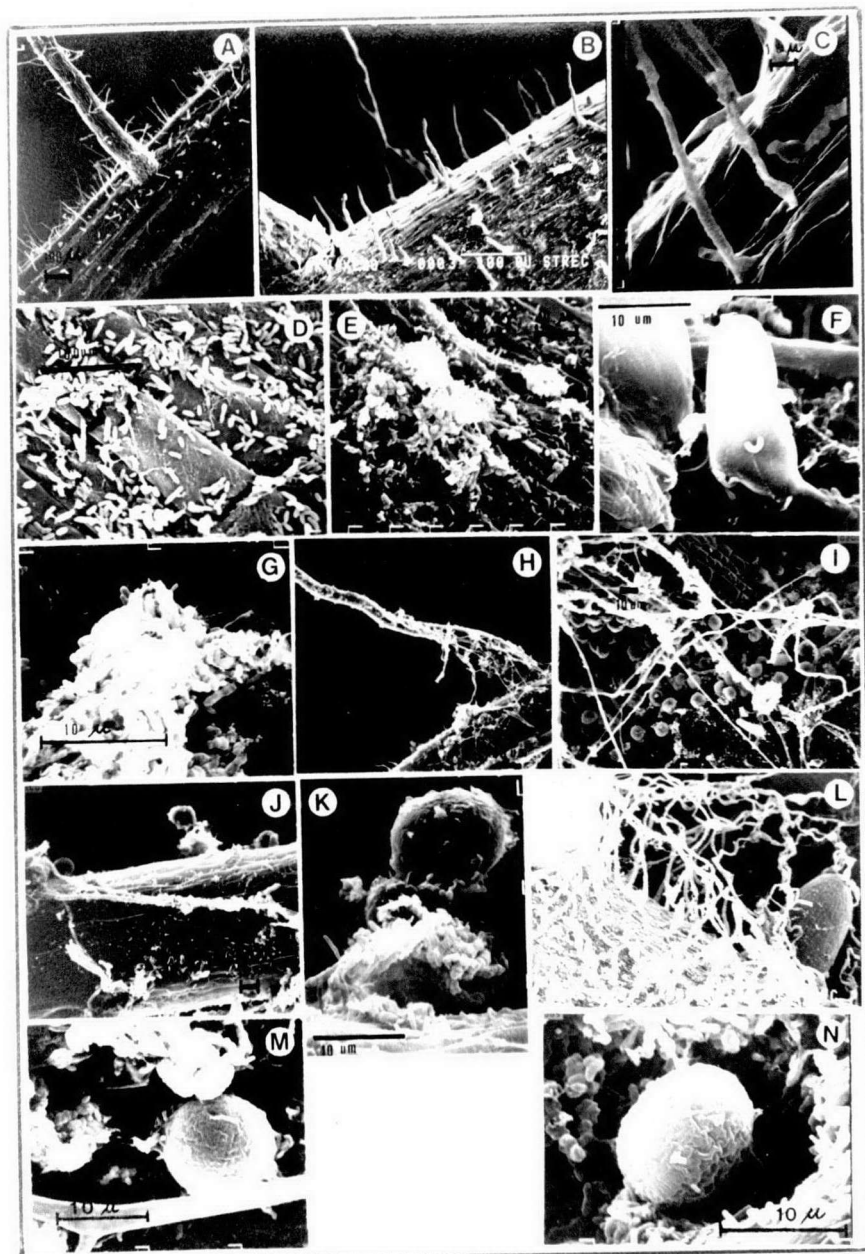
showing a few micronodules cut in halves together with other intact micronodules on the root surface. The content of micronodule looks like agglutinated bacteria wrapped in thin film surround by loosely attached bacteria adhered to the epidermal cells of root. More details are demonstrated in the transmission electron micrographs of rice root ultra-thin sections. Fig. 5A shows a typical cross section of seedling root (7-day-old), showing epidermal cells, where their characteristics are marked by the electron dense outer periphery (Fig. 5B). Cells in the third layer(exodermis) were used as markers because of their thick cell wall to locate epidermal cells on grids (Fig. 5B).

In plant-bacterial association, e.g. rice RD7 and *Klebsiella sp.* R17, the attachment site is clearly shown to be the electron-dense layer on the outer-periphery which are known to be glycocalyx of both bacteria and rice root (Fig. 6A-F). Glycocalyx, which seen to be globular glycoprotein (short arrow head in Fig. 6A) and fibrous polysaccharide (long arrow head in Fig. 6B - E), can not be identified to its origin whether from bacteria or rice root. In addition, some bacteria are seen within the epidermal and cortical

Figure 4   Scanning electron micrographs of a freeze-
fractured   root   sample showing the ultra-structure   of
micronodules.

A   The   cross section of seedling   root   showing
         crust of associative R17.

B   The   cross section of a micronodule   attached
         on the rhizoplane.

C   Intact   micronodules   embedded   in   bag-liked
         structure.

D   The cross section of micronodules   surrounded
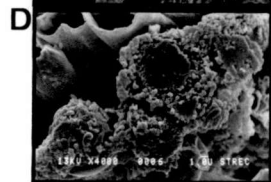   by crust of aggregated bacteria.
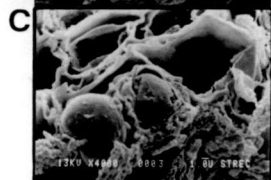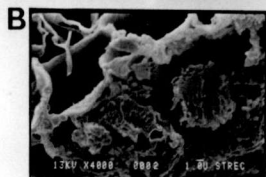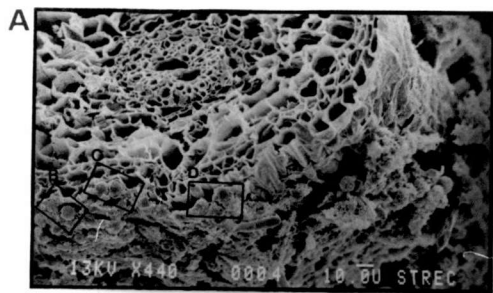
Figure 5   Cross-section of rice seedling-root (7-day-old) and 2 markers used to locate epidermal cells are indicated.

A   Light micrograph of the cross-section of rice root (1000 x). Long arrow head points to exodermis located on the third layer inwards with thick cell wall, used as the marker to specif the epidermal cells on grid.

B   Transmission   electron   micrograph   shows enlarged view of epidermal cells with details on the outer periphery (short arrow head) in the neighborhood of exodermis (long arrow head).
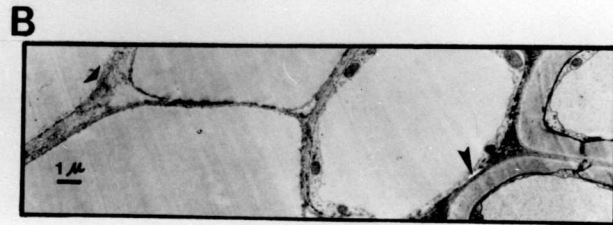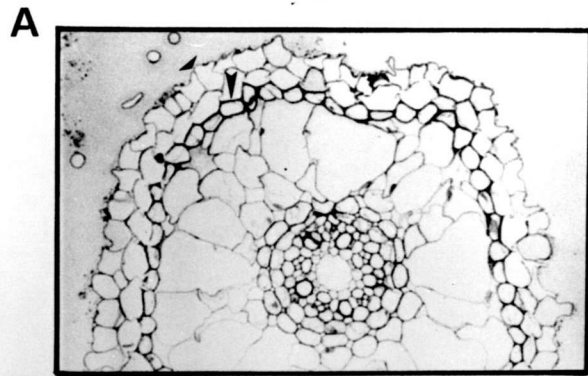
A

B

1 μ

Figure 6   Transmission electron micrographs of rice

(cv.RD7) seedling root in association with *Klebsiella*

sp. R17.

A - F   Cross—section of micronodules   showing

attachment site on the outer periphery of

epidermal cells and electron dense materials

that involve in the micronodule formation.

These electron dense materials so-called glycocalyx

are demonstrated as globular glycoprotein (short

arrow head) and fibrous polysaccharide (long

arrow head).

G   In some area bacteria (R17) are observed in

epidermal cells.
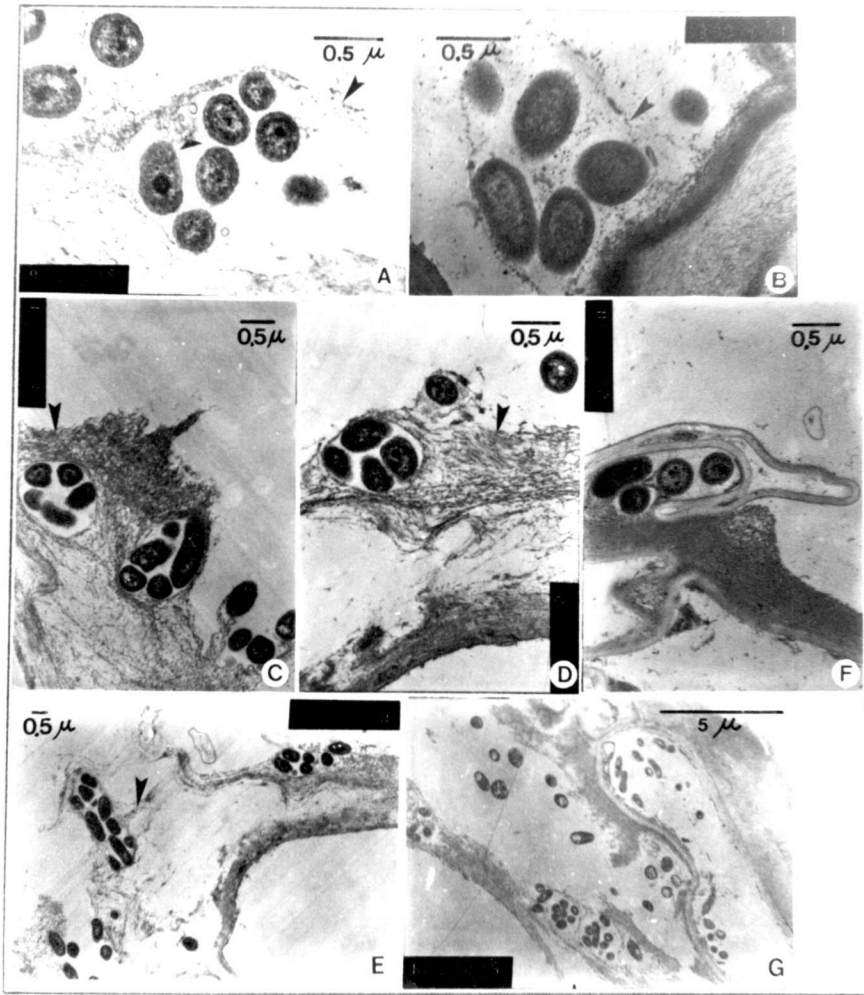
layers without damaging of the epidermal cell wall (Fig. 6G).

3.1.4 Effect of enzyme treatment on the micronodules. In order to test the nature of materials involved in micronodule formation, the micronodulated root samples immersed in buffer without any added enzyme for 24 h were compared with similar samples but treated with different enzymes solutions. No change of micronodule structure is observed in control samples under epi-fluorescence microscopy (Fig. 7A) and scanning electron microscopy (Fig. 8A). Treatment of root samples with 1 unit β-N-acetyl-D-glucosaminidase resulted in shrinkage of the membrane-bound micronodules (Fig. 7B and 8B). The shrinkage of micronodules can be observed also in the root samples treated with 0.2 unit neuraminidase (Fig. 7C and 8C). The diminished in size of micronodules and the liberation of free bacteria from micronodule structure were observed after treatment of the root samples with 10 mg. ml^{-1} β-glucosidase (Fig. 7D and 8D) or 10 mg.ml^{-1} trypsin (Fig. 7E and 8E). It is noted that β-N-acetyl glucosaminidase, neuraminidase and β-glucosidase are enzymes which break down glycosidic linkages and trypsin is enzyme which

Figure 7 Epi-fluorescence micrographs of micronodules of R17 on rice (cv.RD7) seedling root showing the effect of enzymes on micronodules structure.(Magnification x 450)

A   No changes in micronodule structure incubated in PBS.

B   Shrinkage of micronodules due to incubation with 1 unit β-N-acetyl-D-glucosaminidase.

C   Shrinkage of micronodules due to incubation with 0.2 unit neuraminidase.

D   Diminished size of micronodules due to incubation with 10 mg.ml^{-1} glucosidase.

E   Diminished size of micronodules and some liberated R17 due to incubation with 10 mg.ml^{-1} trypsin.
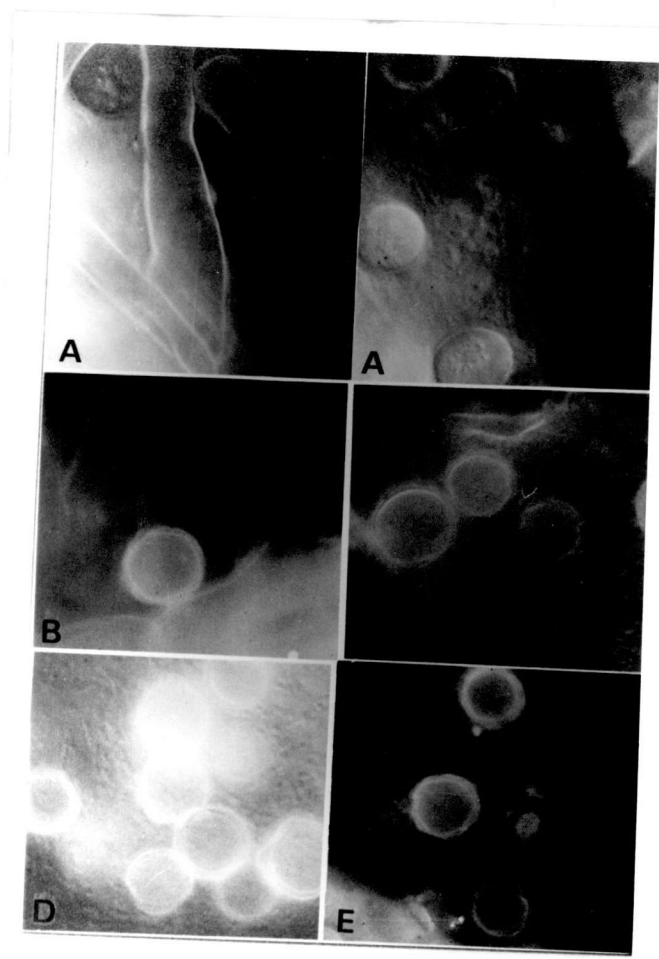
Figure 8   Scanning electron micrographs of micronodules

of R17 on rice (cv.RD7) seedling root showing the effect

of enzymes on micronodule structure.

A   No changes in micronodule structure   incubated

           in PBS.

B   Shrinkage   of micronodules due   to   incubation

           with 1 unit β-N-acetyl-D-glucosaminidase.

C   Shrinkage   of micronodules due   to   incubation

           with 0.2 unit neuraminidase.

D   Degradation of micronodules due to   incubation

           with 10 mg.ml^{-1} glucosidase.

E   Degradation   of micronodules and some liberated

           R17 due to incubation with 10 mg.ml^{-1} trypsin.
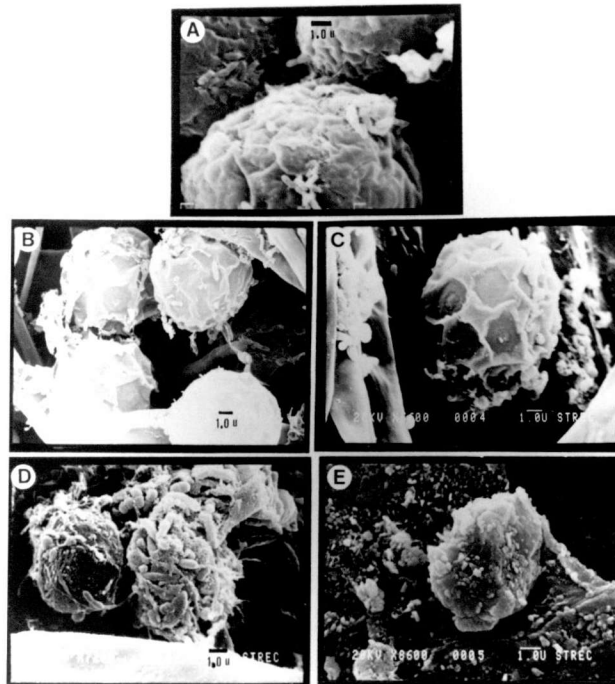
cleave peptide bond. Those enzymes can affect the structure of microndules formed by associative nitrogen fixing bacteria (R15 and R17) on rice root (cv. RD7). These results should indicate the role of glycoprotein in micronodule formation.

3.1.5 Micronodules and nitrogen-fixing activity. From the previous results, micronodules were detected in the R15 or R17 inoculated rice seedling (cv.RD7) after 36 h. Two questions arise 1) whether these phenomena occur only in rice RD7 inoculated by R15 or R17 or any variety of rice and any associative bacteria and 2) whether the formation of micronodules is necessary for induction of nitrogen fixing activity. In order to solve these questions, different varieties of 7-day-old rice seedlings were inoculated with various reference bacteria using similar procedures as described previously. Samples from the same set of tubes were observed for the presence of micronodules, and assay for nitrogenase activity by acetylene reduction activity (ARA). Table 5 shows that micronodules can be observed on roots of rice cv. HCCMM inoculated by *Klebsiella oxytoca* NG13, *Klebsiella sp.* R15 and *Klebsiella sp.* R17. In addition, the rice cv. HCCMM *per se* produced

Table 5 Micronodule formation and nitrogen-fixing activity (ARA) of different rice varities in association with various reference bacteria.

Micronodules are presented as : + means more than 2 nodules on 1 mm long root,

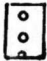- means less than 2 nodules on 1 mm long root

ARA are presented as mean $\pm$ SD from 3 replicates of 9 plants on day 3 after inoculation except RD7 from 10 replicates of 30 plants. ND = not determined

Bacterial strain	Rice varieties											
	None		HCCMM		RD5		RD7		IR42		IR58	
	Micro-nodule	ARA $\mu mol.tube^{-1}.d^{-1}$	Micro-nodule	ARA $\mu mol.tube^{-1}.d^{-1}$	Micro-nodule	ARA $\mu mol.tube^{-1}.d^{-1}$	Micro-nodule	ARA $\mu mol.tube^{-1}.d^{-1}$	Micro-nodule	ARA $\mu mol.tube^{-1}.d^{-1}$	Micro-nodule	ARA $\mu mol.tube^{-1}.d^{-1}$
None	-	0	-	72.2 ± 31.9	-	0	-	0	-	0	-	0
K 12	-	0	-	58.3 ± 28.1	-	0	-	0	-	0	-	0
M5al	-	0	-	67.4 ± 19.9	-	40.9 ± 34.3	-	17.5 ± 20.1	-	0	-	0
NG 13	-	0	+	76.1 ± 31.0	+	17.5 ± 6.1	+	68.9 ± 13.7	-	0	-	0
R15	-	0	+	43.6 ± 6.0	+	83.7 ± 19.9	+	77.6 ± 32.2	-	0	-	0
R17	-	0	+	101.4 ± 19.0	+	31.6 ± 10.5	+	26.9 ± 13.2	-	0	-	0
H 8	-	0	-	86.2 ± 18.2	-	43.9 ± 30.1	-	ND	-	0	-	0
FS	-	0	-	144.1 ± 102.6	+	68.0 ± 38.5	+	ND	-	0	-	0

ethylene which did not significantly increase in association with any nitrogen-fixing bacteria or *E. coli* (control). Inoculation of rice cv. RD5 and RD7 indicate that strains NG13, R15, R17 and *Azospirillum lipoferum* FS induce the formation of micronodules along with significant nitrogenase activity. The free-living diazotrophic bacteria, *Klebsiella pneumoniae* M5a1 inoculated to rice cv. RD5 and RD7 show only nitrogenase activity without any association and micronodules formation. As is M5a1, *Pseudomonas* H8 inoculated to rice RD5 show only ARA . In control experiments, inoculation of *E. coli* K12 and non-inoculated rice RD5 and RD7 yield neither micronodules nor nitrogen-fixing activity. For all bacterial strain tested, whether inoculated or non-inoculated IR42 and IR58 are free from associative micronodules and significant nitrogen fixation.

When the level of nitrogenase activity in a modified spermosphere model consisting of rice RD7 in association with either M5a1, NG13, R15 and R17 was followed continuously after inoculation. Fig. 9 demonstrates that merely associative nitrogen-fixer NG13, R15 and R17 cause a dramatical increase in nitrogenase activity per tube per day. The increase is

Figure 9   Nitrogen-fixing activity (ARA) of rice RD7 in association with various bacteria.

The level of ARA in hydroponic culture of rice RD7 inoculated with either *Klebsiella pneumoniae* M5a1 (▨), or *Klebsiella oxytoca* NG13 (☐) , or *Klebsiella sp.* R15 (▦), or *Klebsiella sp.* R17 (▤) was followed every day after inoculation. Vertical bars represent the standard deviation of the mean from 10 replicates of 3 plants.
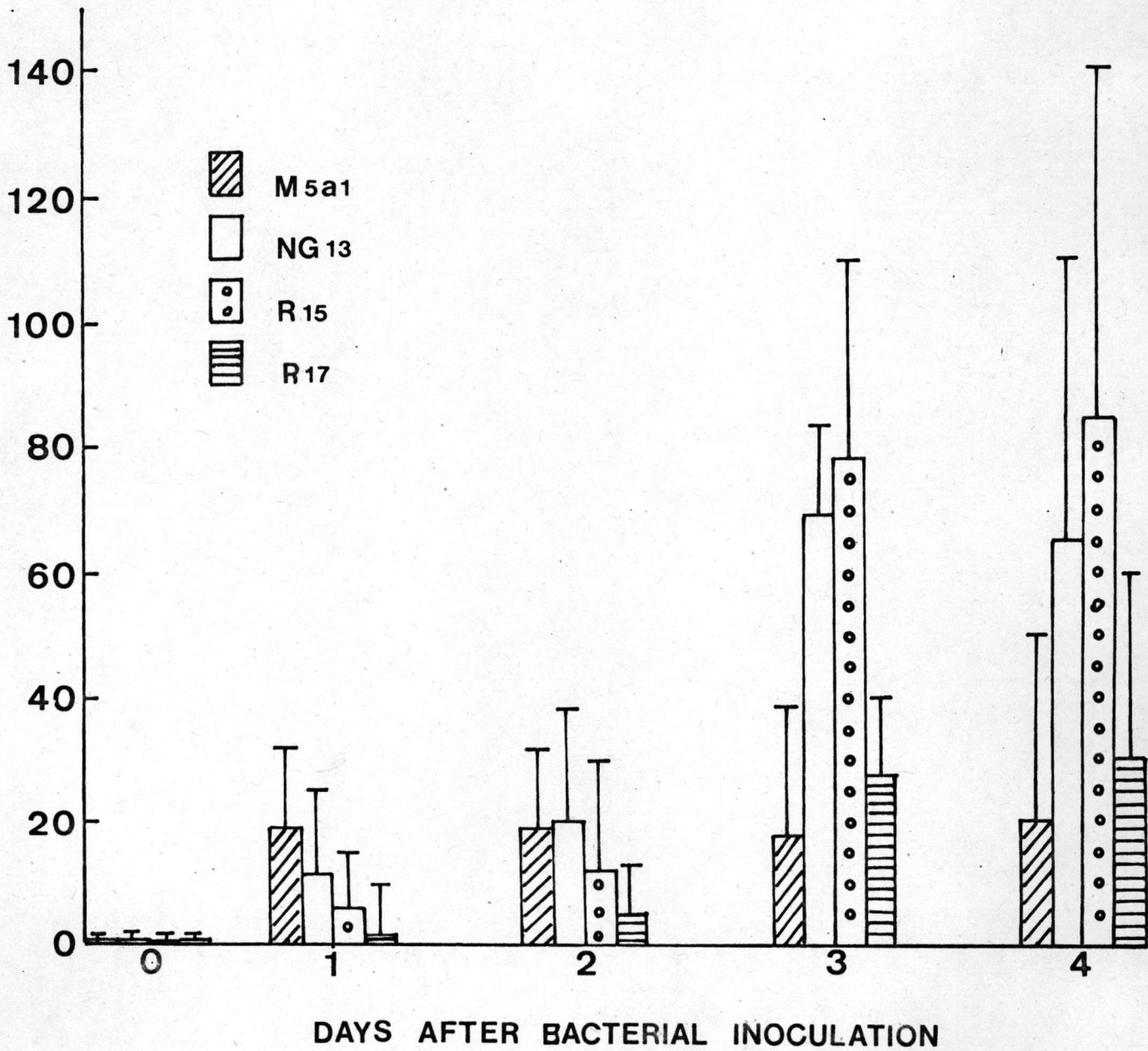
larger than 2-fold on day 3 after inoculation. Inoculation of M5al, the free-living diazotroph shows increasing nitrogenase activity on day 1 and remains constant all through 4 days. It is noted that a sharp increase in the nitrogen-fixing activity induced by the associative NG13, R15 and R17 can be detected after extensive formation of micronodules.

The results in Table 5 also suggest that there are somewhat better complementary pairing between bacterial strain R15 and rice cv. RD5 and RD7 for the consequent micronodules formation and associative nitrogen fixing activity comparing to cv. IR42 and IR58. This complementary pair between bacteria and rice may be generated by several mechanisms, however one of the possible associative factors, the rice lectin will be extensively studied in this research.

3.2 Free lectin in root exudate.

In order to test the role of lectin in the association between nitrogen-fixing bacteria (R15 and R17) and rice (cv.RD7), root exudate was prepared from 7-day-old seedling of rice RD7, IR42 and IR58, and

compared for the hemagglutination activity of lectin. It is clearly shown in Table 6 that lectin excreted in the root exudate of rice cv. RD7 is several hundreds-fold higher than IR42 and IR58. In addition, the amount of dry matter of root exudate from IR42 and IR58 are only 3 - 5 % of the root exudate from RD 7.

3.3 Bound lectin on epidermal cells of rice root.

Rice lectin has been known to bind specifically to GlcNAc, so ^{14}C-GlcNAc can be used as the specific probe to detect bound lectin on the epidermal cell of rice root. The ^{14}C-GlcNAc-incorporation in the root of rice RD7 after 2 h incubation should include not only specific binding of sugar to bound lectin on epidermal cells, but also non-specific binding and sugar uptake into the root cells. In order to determine only specific binding of ^{14}C-GlcNAc to bound lectin on epidermal cells of root, the total ^{14}C-GlcNAc incorporation in pre-labelled roots were subjected to competitive binding with various 200-fold excess non-labelled sugar competitor. Table 7 shows that GlcNAc, the specific hapten of rice lectin, significantly

Table 6   Lectin in root exudate of rice.

Root exudate were prepared from 7-day-old rice seedlings of different varieties, RD7, IR 42 and 58 as described in Methods 2.13.

Root exudate (105 plants)	Source of root exudate		
	RD7	IR 42	IR 58
Total dry matter (mg)	107.2	3.0	5.3
Per cent w/w protein in dry matter	43.0	80.4	28.0
Lectin (HU/mg dry matter)	64	8	8
Total lectin (HU/105 plants)	6,860.8	24.0	42.4

(P<0.01) chase specific ^{14}C-GlcNAc binding to bound lectin on epidermal cells 2-fold higher than other non-specific sugar competitors , mannosamine, glucosamine and glucose. When the bound lectin on rice epidermal cells was calculated in term of bound ^{14}C-GlcNAc by subtracting the radioactivity of ^{14}C-GlcNAc chased out by GlcNAc (8.47 x 10^4 dpm.mg^{-1} DNA) with the average radioactivity of ^{14}C-GlcNAc chased out by other 3 non-specific sugar-competitors (3.13 x 10^4dpm.mg^{-1} DNA), the result was 5.34 x 10^4 dpm.mg^{-1} DNA or 4.16 μmol.g^{-1} DNA or 0.92 μg.mg^{-1} DNA.

Under this condition the sugar uptake into the root cells, calculated by subtracting the radioactivity of total ^{14}C-GlcNAc incorporation into root cells (17.45x10^4dpm.mg^{-1}DNA) with specific and nonspecific binding of ^{14}C-GlcNAc on root epidermal cells, was 9 x 10^4 dpm.mg^{-1} DNA.

These results indicate that in the rice rhizosphere, the lectins are liberated in root exudate (3.2) as well as bound to the epidermal cells of root surface (3.3).

Table 7   Specific binding of ^{14}C GlcNAc to bound lectin on epidermal cells of rice root.

Pre-labelled rice roots with 0.5 μCi ^{14}C-GlcNAc for 2 h. (zero time for control), were incubated in sugar competitor solutions, the radioactivity in both sugar solution and remained in root tissue were measured and results were expressed in term of dpm/mg DNA.

Sugar competitor	No. of exp.	sp. radioactivity in sugar soln		sp. radioactivity remained in root 10^{-4} dpm/mg DNA	Total sp. radioactivity 10^{-4} dmp/mg DNA
		10^{-4} dpm/mg DNA	% of total		
PBS (control)	3	0	0	0	0
GlcNAc	3	8.47 ± 1.05* a	44.5	10.55 ± 2.73 a	19.02 ± 1.73 a
ManN	3	3.61 ± 0.37 b	23.4	11.68 ± 2.88 a	15.29 ± 2.59 a
GlcN	3	2.59 ± 0.39 b	13.4	16.79 ± 0.54 a	19.38 ± 0.92 a
Glc	3	3.18 ± 1.65 b	19.7	12.94 ± 2.16 a	16.12 ± 1.63 a
					avg 17.45 ± 2.45

*numbers followed by the same letter in each column are not significantly different at $P < 0.01$ as shown in Appendix 1.

3.4 Purification of rice lectin.

The important step for rice lectin purification was the step of affinity chromatography based on specific binding of rice lectin to GlcNAc. Preparation of affinity gel with high rice lectin binding capacity was attempted by coupling epoxy-Sepharose 6B with equal volume of GlcNAc at various concentrations (50 to 180 mg.ml^{-1} in 0.1 N NaOH) according to Vretbald (1976). Table 8 shows that 100 mg.ml^{-1} GlcNAc resulted in affinity gel with the highest lectin binding capacity close to the value obtained with Selectin 1.

Chitin, the naturally occuring polymer of GlcNAc, when ground and packed into a column serves both as matrix and ligand in an affinity chromatographic column. On separation of rice lectin, the chitin column shows maximum lectin-binding capacity about 4-fold higher than Selectin 1 (Table 8).

The affinity chromatographic profile of rice bran extract (AS-60) on prepared Sepharose 6B-GlcNAc gel eluted with 0.2 M GlcNAc (Fig. 10) shows only one protein peak that also coincided with lectin hemagglutination activity peak. Similar profile was obtained from Selectin 1 column eluted with 0.2 M, GlcNAc (Fig. 11).

Table 8   Rice bran lectin binding capacity of prepared GlcNAc-Sepharose 6B affinity gel, Selectin 1 and chitin column.

GlcNAc-Sepharose 6B affinity gel was prepared with varying concentration of GlcNAc in 0.1 N NaOH from 50 mg/ml to 100, 140 and 180 mg/ml when coupling to equal volume of wet epoxy-Sepharose 6B gel.

Affinity gel	lectin binding capacity (mg/5 ml gel or 1 g chitin)
Prepared GlcNAc-Sepharose 6B affinity gel	
- 50 mg/ml GlcNAc	1.16
- 100 mg/ml GlcNAc	2.40
- 140 mg/ml GlcNAc	1.02
- 180 mg/ml GlcNAc	0.80
Selectin 1[R]	2.80
Chitin	11.09

Figure 10 Purification of rice lectin on epoxy-Sepharose

B-GlcNAc column.

Loading of AS-60(15 ml) onto a GlcNAc-Sepharose 6B
column (1.2x6 cm) at a flow rate of 15 ml.h^{-1}. Unbound
proteins were completely washed out with PBS. Lectin,
the affinity-bound protein was then eluted with 0.2 M
GlcNAc in PBS and collected in 2.5 ml fractions.
Protein profile was monitored by A_{280} (●————●).
The protein fractions were freed from sugar hapten by
passing through Sephadex G-25 column,and were assayed
for lectin activity by hemagglutination test (▲————▲).

Epoxy Sepharose–6B–Glc N Ac Column

Apply sample

A_{280}

PBS

0.2 M Glc N Ac

HU

Fraction number
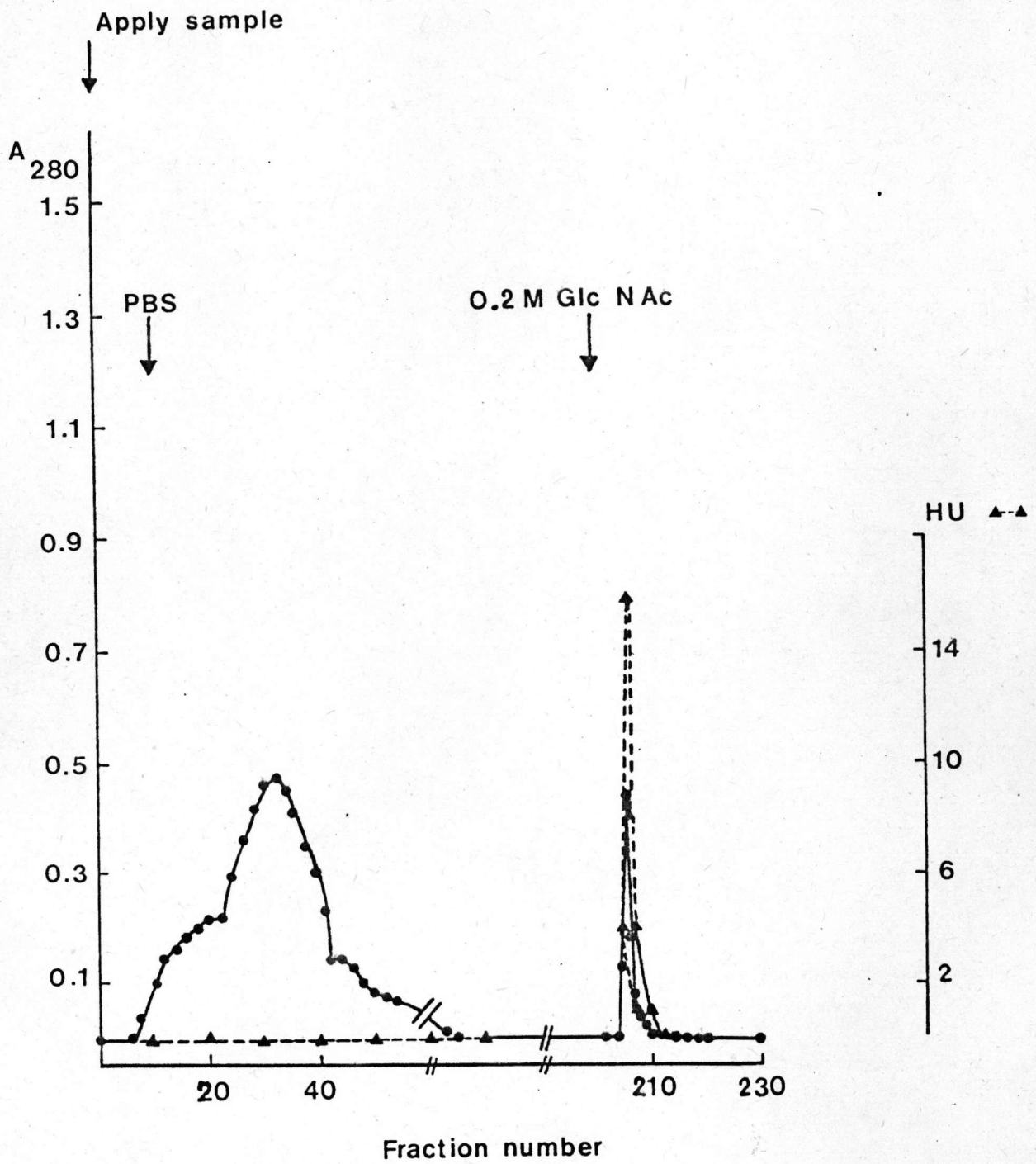
In the case of chitin affinity column, 0.2 M GlcNAc is not sufficient to elute rice bran lectin strongly bound to chitin, either 0.05 N HCl or 1% w/v chitin hydrolysate (oligomers of GlcNAc) must be used, resulting in different patterns as shown in Fig. 12 and 13. Chitin hydrolysate (1% w/v) specifically elutes only one peak of protein showing hemagglutination activity of lectin, whereas 0.05 N HCl elutes also other proteins without lectin activity.

Taking into account of these results, as well as the easier and cheaper preparation of chitin column comparing to Sepharose 6B-GlcNAc affinity gel, further purification of lectin from bran, embryo and root are performed on chitin column eluted with 1% w/v chitin hydrolysate.

The specific activity of purified lectin either from bran, embryo or root after the final step of affinity chromatography is similar about 100 $HU.mg^{-1}$ protein (Table 9). It is noted that very little lectin activity (<10%) was lost during this scheme of purification.

Figure 11 Purification of rice lectin on Selectin 1 column.

Sample of AS-60 (15 ml) was loaded at a flow rate of 15 ml.h^{-1}. Unbound proteins were completely washed out with PBS as monitored by A$_{280}$ (●——●). The affinity bound lectin was then eluted with 0.2 M GlcNAc in PBS and collected in 2.5 ml fractions. Lectin was determined by hemagglutination assay (▲——▲) in the protein fractions which already passed through Sephadex G-25 to remove sugar hapten.
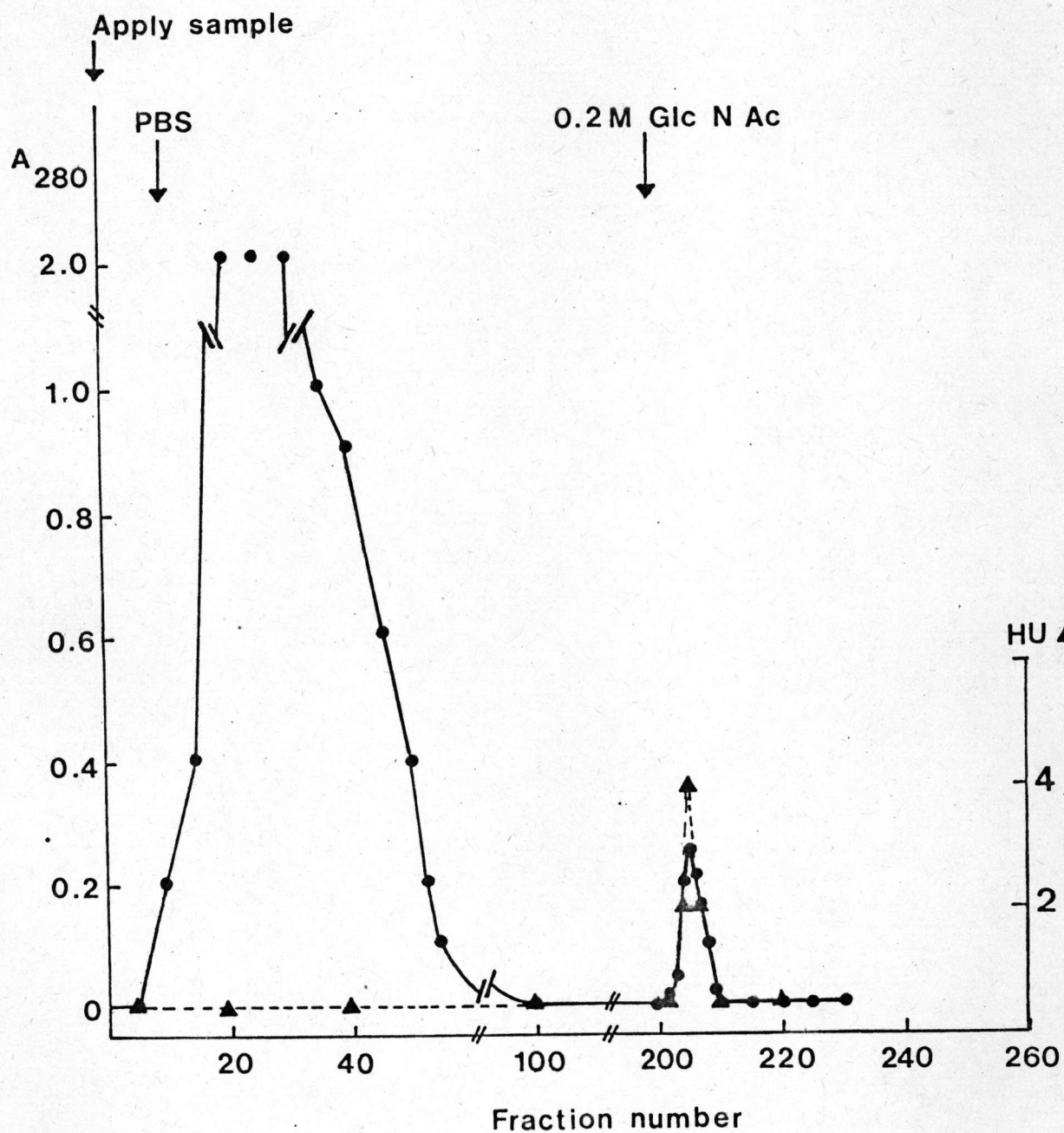
Selectin I Column

Figure 12 Purification of rice lectin on chitin column

eluted with 0.05 N HCl.

Extracted sample of AS-60 (20 ml) was loaded into a

chitin column (2x30 cm) at the flow rate of 15 ml.h^{-1}.

The unbound proteins were completely washed out with

PBS and followed by 0.1 M phosphate buffer pH 7.4.

The adsorbed proteins were then eluted with 0.05 N HCl.

The protein and lectin activity were followed by A_{280}

(o———o) and hemagglutination assay (▲———▲) respectively.
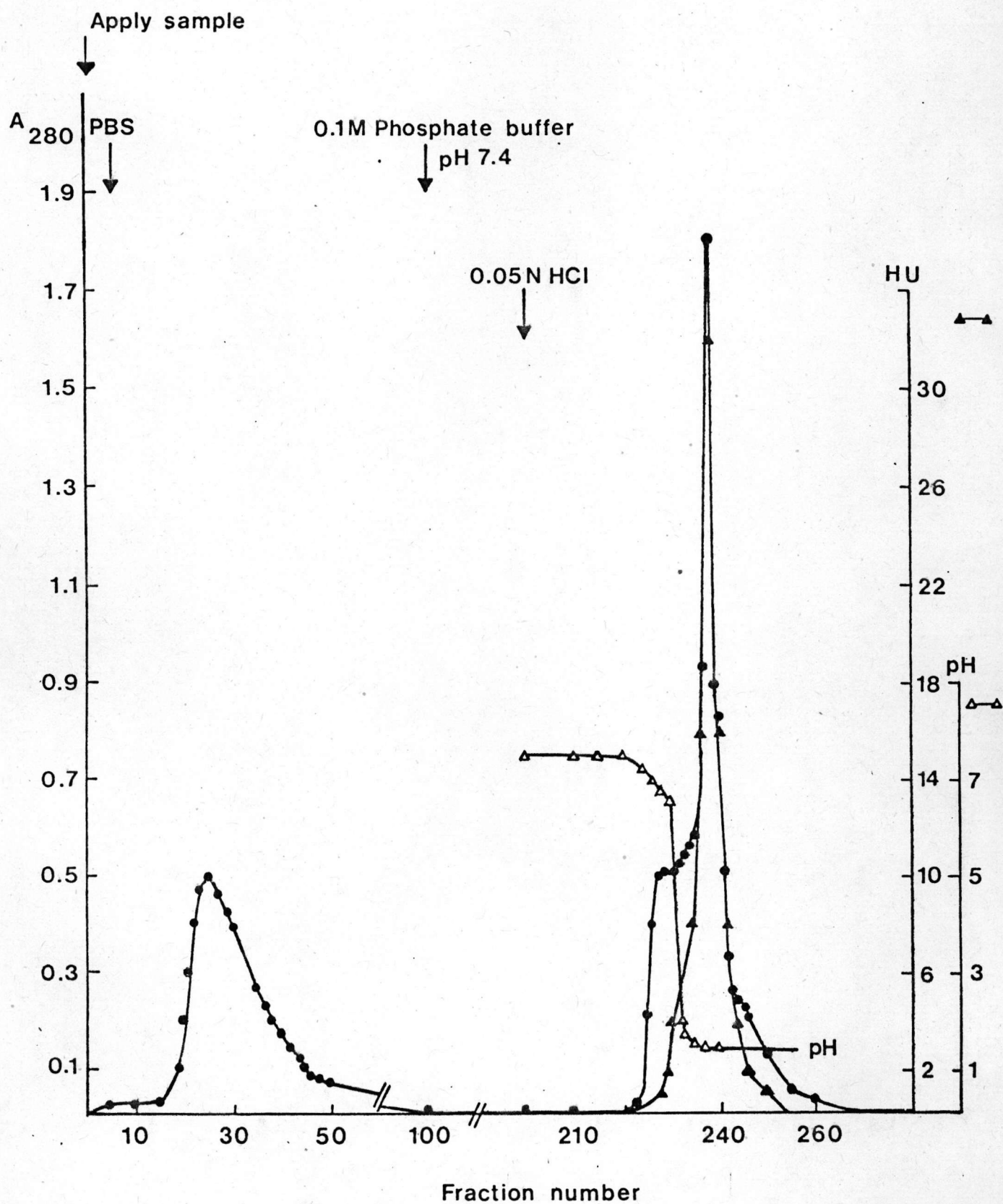
The pH of eluated were recorded (△———△).

Chitin Column

Figure 13 Purification of rice lectin on chitin column eluted with 1% w/v chitin hydrolysate.

Sample of AS-60 fraction (20 ml) was loaded into a chitin column (2x30 cm) at the flow rate of 15 ml.h^{-1}. The unbound proteins were completely washed out with PBS and followed by 0.1 M phosphate buffer pH 7.4. The adsorbed lectin was then eluted with 1% w/v chitin hydrolysate and protein profile was monitored by A$_{280}$ (●——●). These protein fractions were passed through a Sephadex G-25 column and then assayed for lectin activity by hemagglutination test (▲——▲).
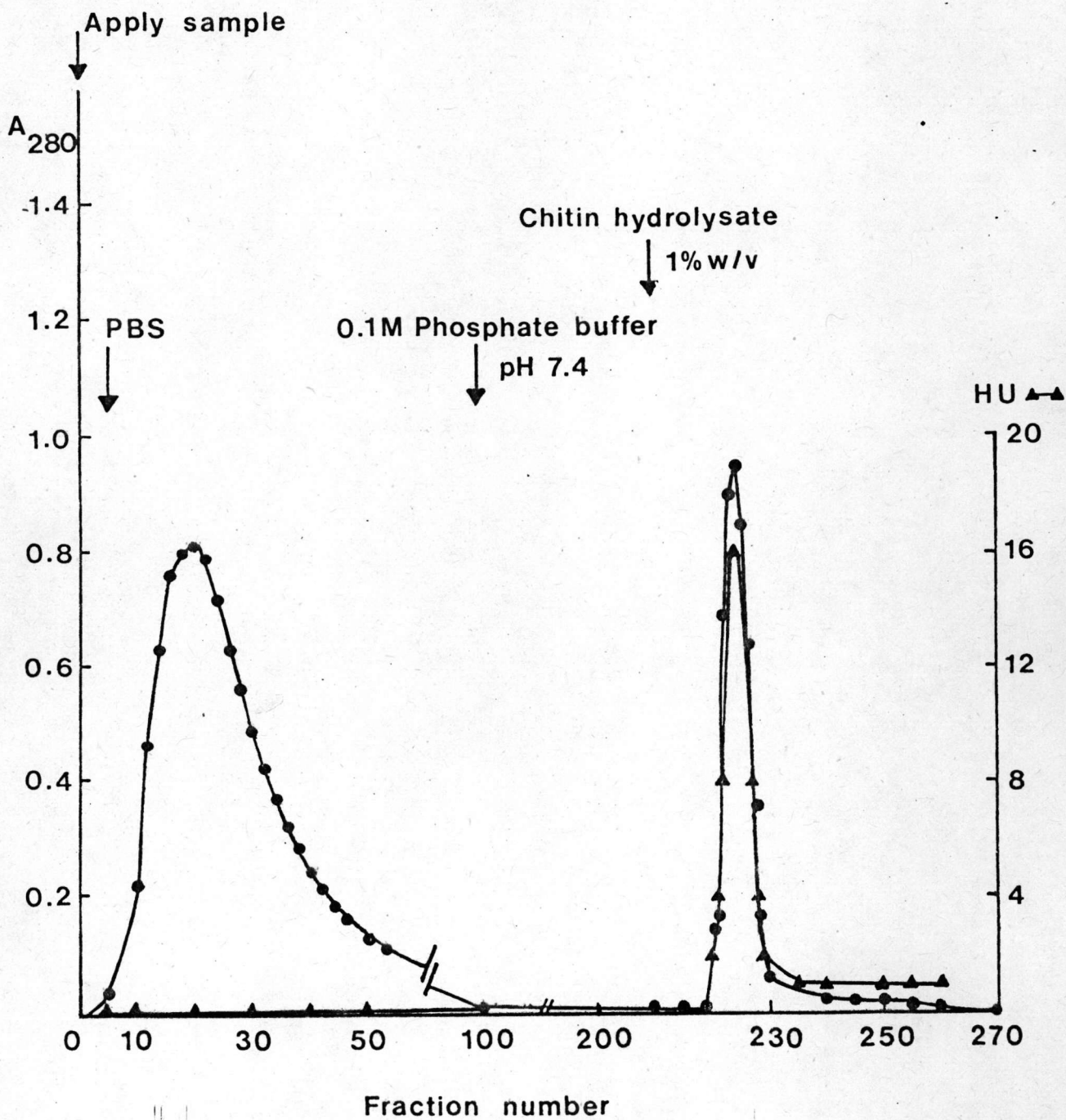
Chitin Column

Table 9   Purification of rice lectin from bran, embryo and seedling root of rice (_Oryza_ _sativa_ RD 7).

Source	Steps of Purification	Total protein (mg)	Total lectin activity (HU[*] x 10^3)	Specific activity (HU/ µg prot.)	Purification -fold	Activity yield (%)
Bran	SF-8	6500	482	0.1	1	100
(200 g)	AS-60	1596	627	.4	5.6	130
	Affinity Chrom.	5.6	549	98.0	1400	114
Embryo	SF-8	1738	722	0.4	1	100
(40 g or 20,000 embryos)	AS-60	1345	640	0.5	1.1	89
	Affinity Chrom.	6.7	684	102.1	242.9	95
Seedling-root	SF-8	950	122	0.1	1	100
(500 g or 24,000 plants)	AS-60	343	146	0.4	3.3	120
	Affinity Chrom.	0.95	108	113.7	874.5	89

[*]HU = Haemagglutinating unit, a reciprocal number of titer

(titer is the highest dilution that causes haemagglutination)

SF-8 = PBS extract after 7020 xg centrifugation

AS-60= 60% Ammonium sulfate precipitation

Affinity Chrom. = Chitin column eluted with 1% chitin hydrolysate.

The purity of lectins prepared from bran, embryo and root are evident by a single band on polyacrylamide gel electrophoreses (Fig. 14) and a symmetrical protein peak on Sephadex G-100 column (Fig. 15).

3.5 Characterization of rice lectin.

3.5.1 Molecular weight. Purified rice lectin from embryo and root show similar molecular weight of 22K on a Sephadex G-100 column (Fig. 15) according to the standard graph constructed from the molecular weight of protein markers and K_{av}.

3.5.2 Subunit molecular weight by SDS-PAGE. The subunit molecular weight of rice lectin from bran, embryo and root after subjected to SDS-PAGE according to Leamli (1970) show only one broad diffusable band of molecular weight around 22-24 K (Fig. 16), suggesting that rice lectin from bran, embryo and root of rice RD7 are more or less similar. However the presence of the broad diffusable band had led the author to repeat SDS-PAGE with modification according to Allore and Barber(1984) using the same lots of purified lectin . stored frozen in a freezer (-4 ^{O}C) for about one month. The essence of modification from the conventional one dimensional SDS-PAGE is to load

Figure 14 Polyacrylamide gel electrophoresis of purified rice lectin.

Lane 1, 50 μg AS-60 fraction from embryo extract.

Lane 2, 50 μg unbound protein fraction after loading AS-60 from embryo on the chitin column.

Lane 3, 50 μg purified embryo lectin eluted from the chitin column with 1% w/v chitin hydrolysate.

Land 4, 50 μg purified root lectin eluted from the chitin column with 1% w/v chitin hydrolysate.

Land 5, 50 μg unbound protein fraction after loading AS-60 from root on the chitin column.
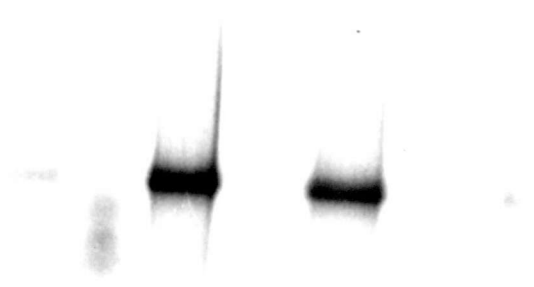
Land 6, 50 μg AS-60 fraction from root extract.

Figure 15 Elution profile of purified rice lectins on Sephadex G-100 column.

Purified lectin from embryo or root (1 ml of 5 mg) loaded on Sephadex G-100 column, equilibrated with PBS and the protein was monitored by absorbancy at 280 nm. The calibration curve of molecular weight and K_{av} was performed from standard protein markers of BSA (68 K), ovalbumin (43 K), α-chymotrypsinogen A (26 K) and lysozyme (14 K). K_{av} is the ratio of (Ve-Vo) to Vi.

Sephadex G-100 Column

Molecular weight x 10^{-4}
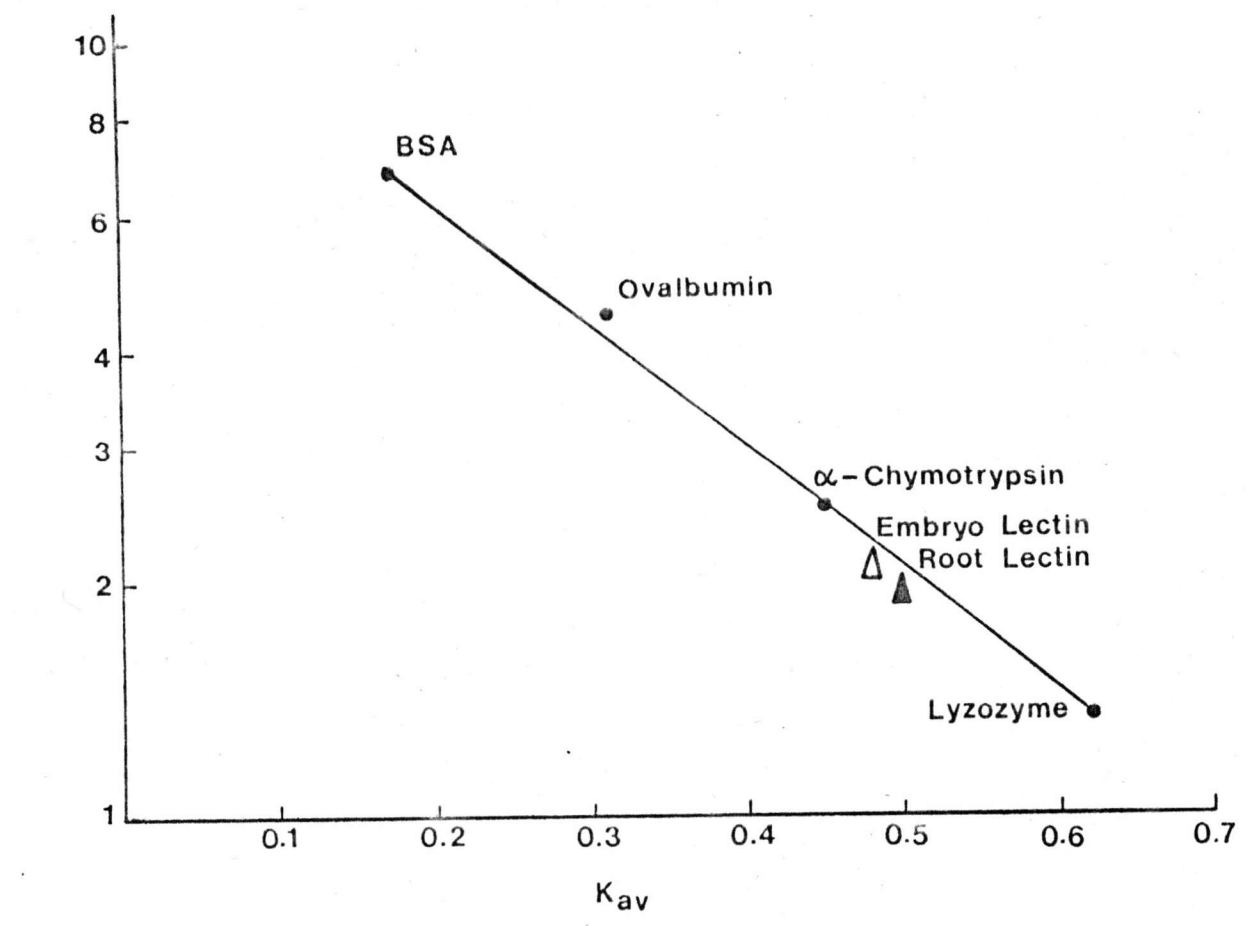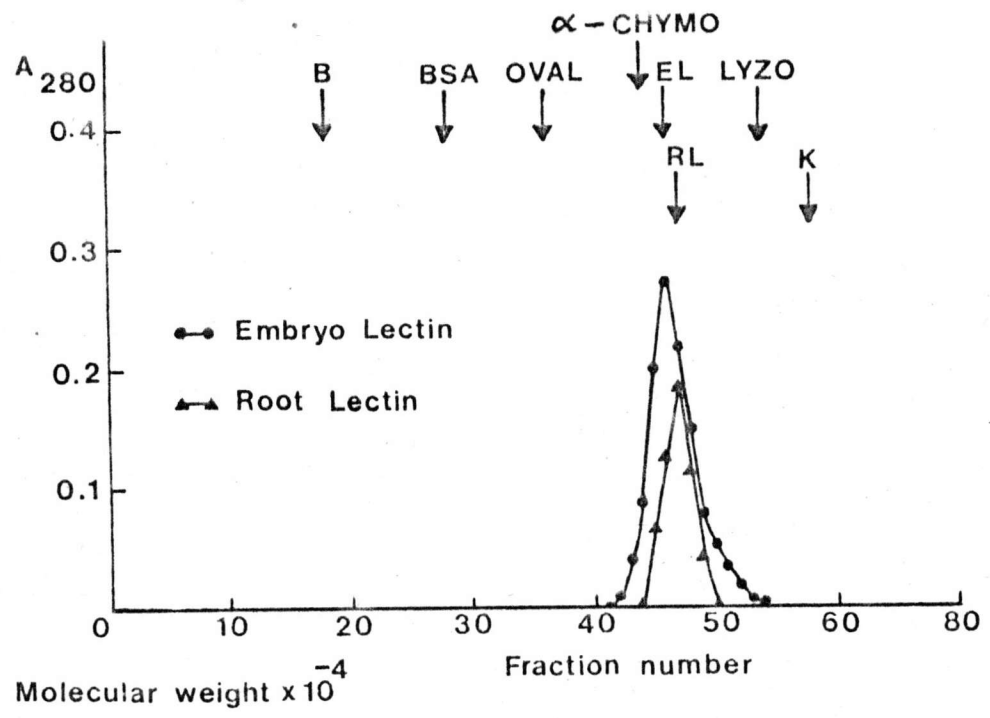

K_{av}

Figure 16 SDS gel electrophoresis of purified lectins.

Bran lectin (BL), embryo lectin (EL) and root lectin
(RL) purified from rice cv. RD7 were treated with
solubilizing medium containing 1% SDS, 4% v/v glycerol,
1% v/v 2-mercaptoethanol in 0.062 M Tris-HCl pH 6.8 and
boiled for 2 min prior to application. In each lane 10
μg of lectin was loaded. In land S, molecular weight
markers which are mixture of bovine serum albumin (68
K), ovalbumin (45 K), pepsin (35 K), trypsinogen (24
K), β-lactoglobulin (18 K) and lysozyme (14 K) were
loaded as reference.
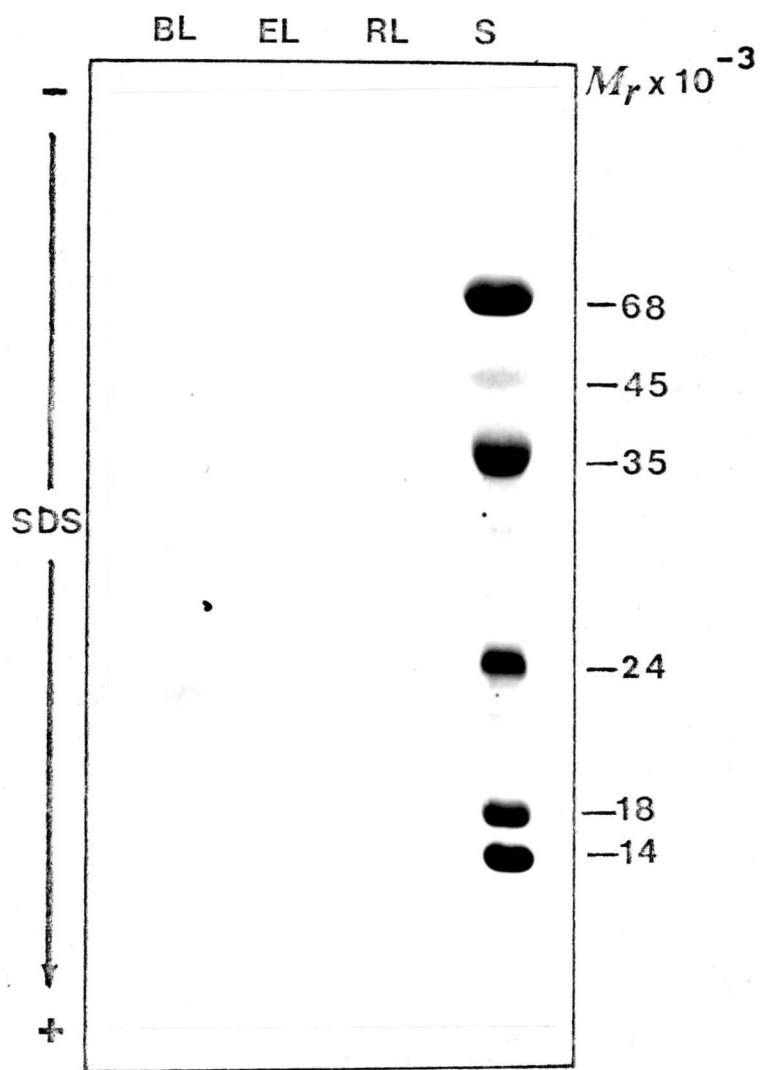
duplicate protein samples containing reducing agent (lanes with plus sign) immediately adjacent to the latter duplicate samples in the absence of reducing agent (lanes with minus sign), and the concentration of reducing age..c, mercaptoethanol(MeSH), was 5% v/v which was 5-fold of the former experiment. In Fig. 17A, root lectin (RL) was loaded 10 μg in each lane which was the equal amount as in the Fig.16, only one major diffusable band of 22K protein is observed in lane 5 (no MeSH) which shift to be 24K in the presence of MeSH (lane 2 and 3). These results agree with those observed in Fig. 16. As the amount of sample loaded on each gel was increased (20 μg for BL and 30 μg for EL), transition of the 22K band to the 24K band in reduced condition is more obvious(Fig. 17A and B), especially in lane 8 which is partly influenced by the "plus" lane shows decreasing density at 22K. This type of transition in apparent molecular weight should be due to the unfolding of an internal disulfide-bonded domain. The 18K protein (lane 10) apparent in reduced condition is not seen in non-reduced lane 7 indicating that 18K protein might be derived from 22K protein. It is clear that 20K protein

Figure 17   SDS-gel electrophoresis of rice lectin in

reduced and non-reduced conditions.

Root lectin (RL=10 μg),   bran lectin (BL=20 μg) and embryo

lectin (EL=30 μg) samples   in (+) lanes   were treated

with   5% v/v mercaptoethanol, whereas those in (-) lanes

were not treated.   Lane 1 and 6 (S) show   standard

molecular   weight   proteins of bovine   serum   albumin

(68   K); ovalbumin   (45 K); α-chymotrypsinogen (26 K);

β-lactoglobulin (18 K), lysozyme (14 K) and cytochrome c.

(12 K).
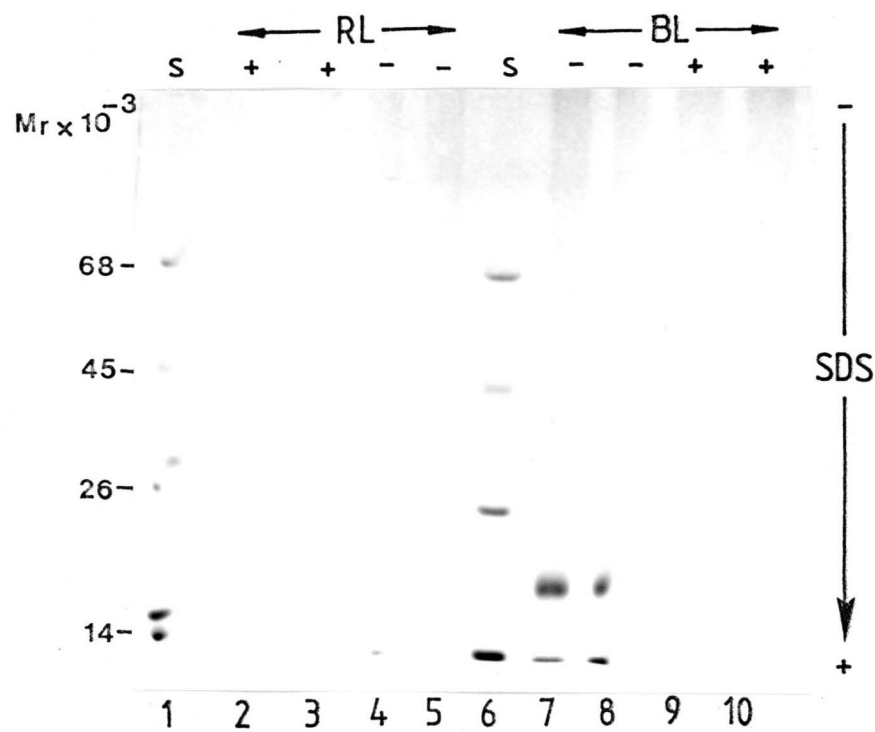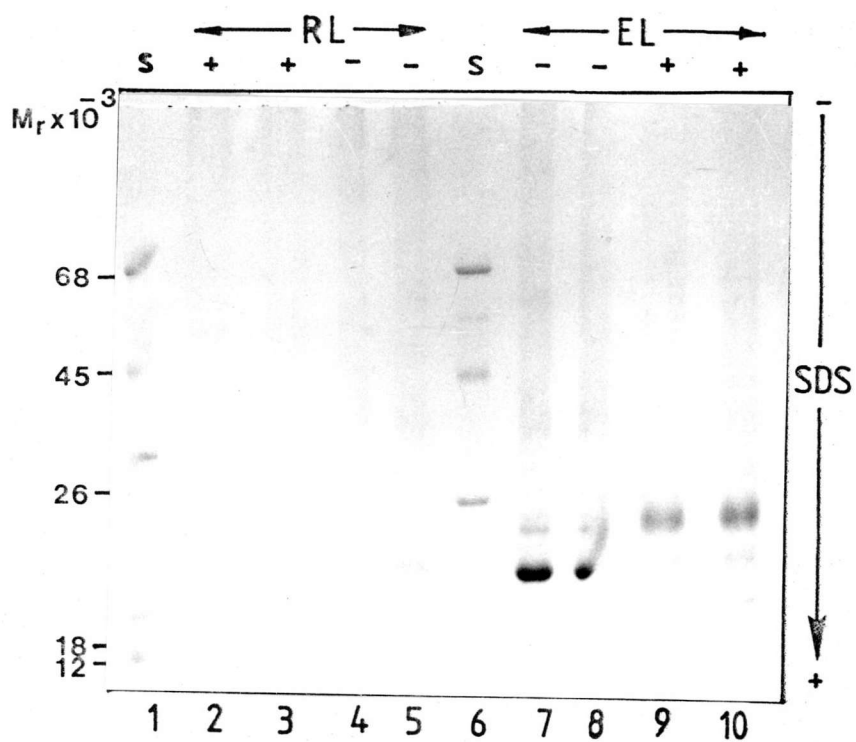
band (Fig. 17 lane 7,8,9,10) is completely unaffected by the presence or absence of reducing agent, thus this polypeptide should not contain inter- or intrachain disulfide bonds.

Apparently, rice lectin from bran, embryo and root exhibit very similar profiles on SDS-PAGE. At least 2 different polypeptides are found in rice lectin, one with inter- and intrachain disulfide bonds in its tertiary structure resulting in different apparent molecular weight of 24K, 22K and 18K depending on the presence of reducing agent and another polypeptide, 20K which is not affected by MeSH.

3.5.3 Isoelectric points of rice lectin.

Isoelectric points of rice lectin from embryo and root are shown to be common in 3 bands of pI 4.5, 4.7 and 5.0, whereas an extra-sharp band of pI 5.05 is observed only in root and merely diffused band of pI ranging from 5.0 to 5.2 is apparent in lane 1 loaded with embryo lectin (Fig. 18).

Figure 18   Isoelectric focusing (IEF) gel eletrophoresis
of embryo and root lectin.

Lane 1 and 2 are 400 μg embryo lectin and 400 μg root
lectin respectively. Standard proteins used as pI markers
are ; ovalbumin (4.7) ; bovine serum albumin (5.2) ;
phosphorylase b (6.4); myoglobin (7.3) and trypsinogen (8.7).

pl   1 2

4.7 -

5.2 -

6.4 -

7.3 -

8.7 -
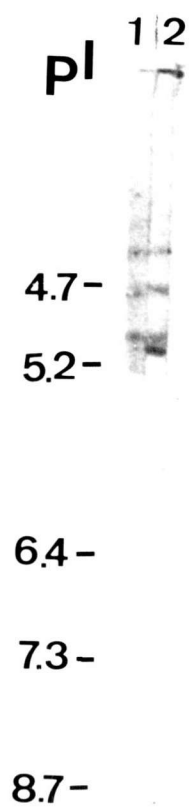
It is of interest to characterize each isoelectric band for its lectin agglutinating activity, therefore another identical but unfixed gel was cut into series of ~2 mm slice, each was extracted with 100 μl 0.9% NaCl for 2 h at room temperature and assayed for its lectin activity per slice as demonstrated in Fig. 19 All major bands in the IEF gel either EL or RL exhibit lectin activity. The presence of 0.2 M GlcNAc inhibits hemagglutinating activity of all these active fractions. These data suggest that they may be as many as 4 isolectins in rice, which might be corresponded with the 4 protein bands (24K, 22K, 20K and 18K) observed by SDS-PAGE (Fig. 16). In order to prove this assumption, two dimensional IEF and SDS-PAGE was conducted as described in Methods 2.29. Fig. 20 shows that isolectins of pI 4.5, 4.7 and 5.0 exhibit the molecular weight of 24K, 22K and 20K respectively, and a very faint spot corresponding to pI of 5.05 around 18K. Thus, the variation in pI of rice lectin isolated from bran, embryo and root of rice (*Oryza sativa* cv.RD7) is conformed with variation in molecular weight polypeptides displayed in SDS-PAGE.

Figure 19 The lectin activity of various isoelectric
bands of embryo lectin and root lectin after IEF gel
electrophoresis.

A duplicate unfixed IEF gel of embryo lectin (A) and
root lectin (B) (~ 2 mm each) were extracted in 100 μl
0.9% NaCl. Lectin activity determined as hemagglutinating
titer is associated with all major bands showing the maximum
lectin activity at pI=5.0.

A.

pI   4.7 5.2   6.4   7.3   8.7

titer

B.

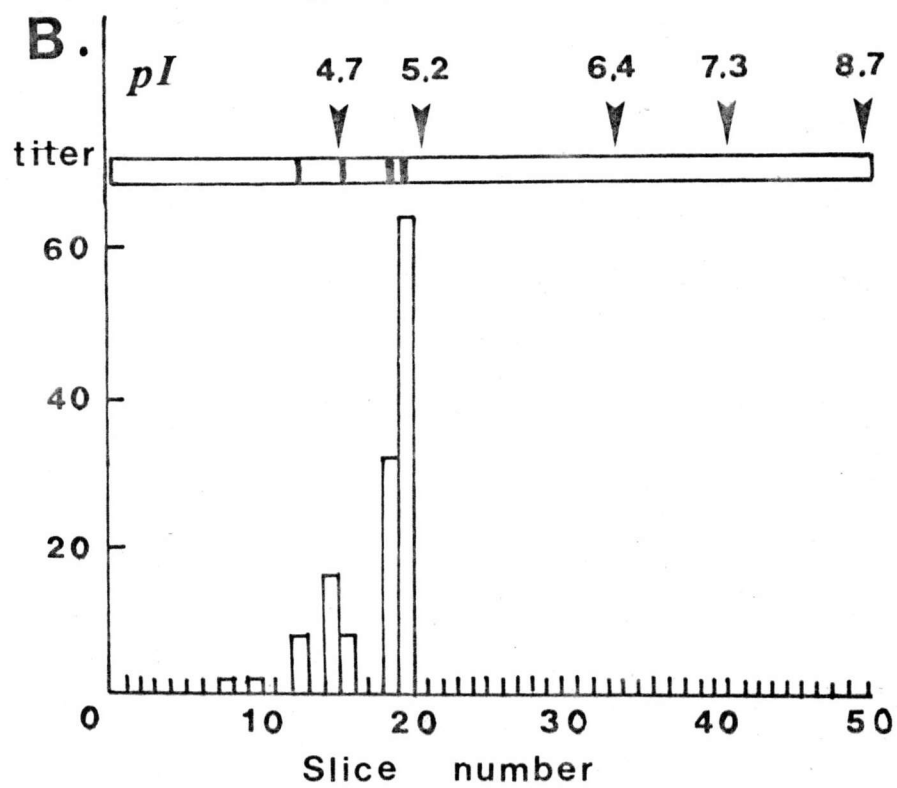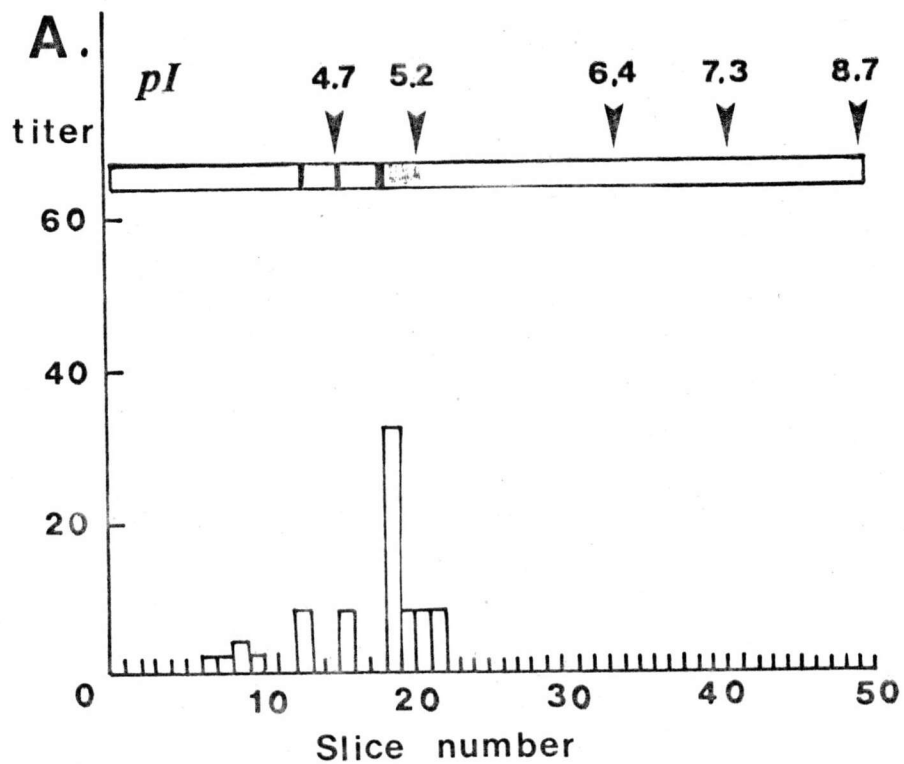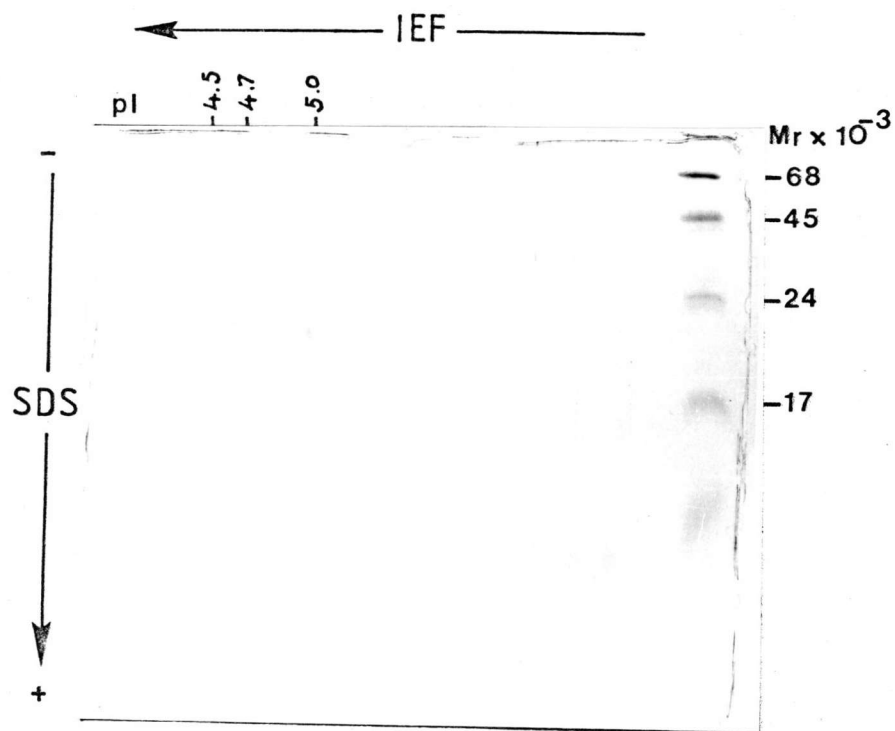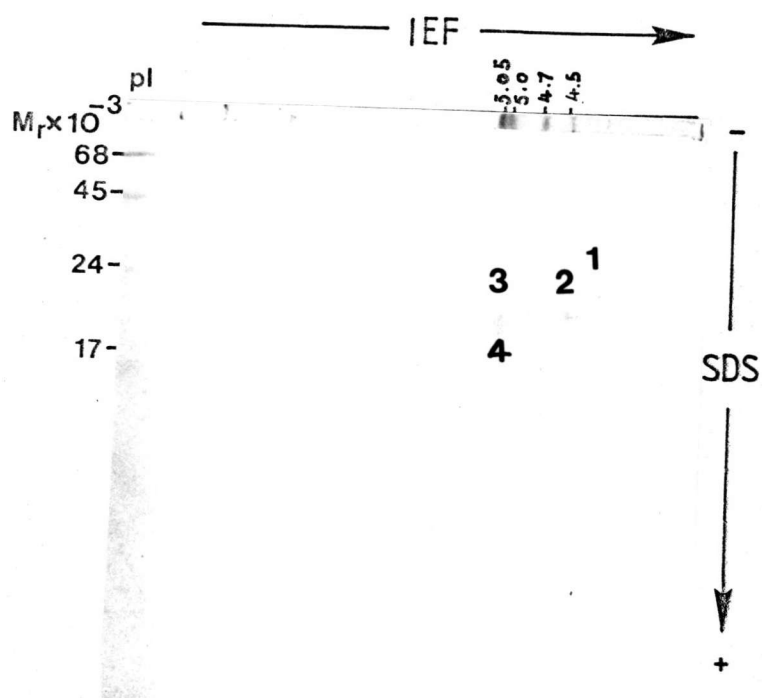pI   4.7 5.2   6.4   7.3   8.7

titer

Figure 20   Protein pattern of IEF-SDS 2-dimensional electrophoresis of rice lectin from embryo(A) and root(B).

Protein was loaded in IEF gel 300 μg in first dimension and then SDS electrophoresis in second dimension. Protein molecular weight markers were : bovine serum albumin (68 K); ovalbumin (45 K); trypsinogen (24 K) and myoglobin (17 K).

A.

B.

3.5.4   Amino acids composition of purified rice

lectin.   To   standardize the   analytical   method   of

amino   acids   composition, pure   wheat   germ   agglutinin

(WGA)   was   used as tested material.   The   amino   acids

composition of WGA calculated by using pure amino   acids

as   standard comparing to that reported by Nagata (1974)

(Appendix B),   suggests   that there   is   some   lost   of

cysteine   during oxidizing step.   Therefore, the   result

was   recalculated by using glutathione   (oxidized   form)

treated   in parallel to sample as standard   for   cysteic

acid, glutamic acid and glycine (Appendix B), and   shown

to correspond with that reported by Nagata (1974).

More or less similar composition of amino acids is

reported here with rice lectin purified from root,   bran

and embryo (Table 10).   The major amino acids in these

three sources of rice lectin molecule are glutamic acid,

cysteic acid and glycine respectively.

Table 10   Amino acids composition of purified rice lectin.

Amino acids	mol % recovered		
	root lectin	bran lectin	embryo lectin
Aspartic acid	7.2	7.4	5.8
Threonine	3.4	3.4	3.0
Serine	6.5	6.7	7.4
Glutamic	13.8	13.9	15.3
Proline	4.8	5.8	4.2
Glycine	9.3	9.5	8.8
Alanine	7.6	7.8	7.0
Cysteic acid	11.2	11.2	11.2
Valine	5.2	4.6	5.3
Methionine	1.9	1.9	2.6
Isoleucine	3.0	2.6	2.7
Leucine	6.3	6.3	6.0
Tyrosine	2.6	2.6	3.8
Phenylalanine	3.5	3.4	3.1
Lysine	3.9	3.8	2.7
Histidine	2.2	2.2	2.0
Arginine	7.7	7.7	9.4

3.5.5   Amount   of   carbohydrate   in   rice   lectin.

Table 11 give values of the carbohydrate content (% w/w)

in   rice lectin purified from bran, embryo and   root   by

comparison to D-glucose or L-arabinose as standard.   The

total   amount   of carbohydrate in rice   lectin   purified

from root, bran and embryo are in the range of   8.1-9.1,

0.9 - 7.5 and 2.8 - 4.5 % w/w respectively.   Control

experiments with known glycoproteins such as fetuin   and

horseradish   peroxidase yield per cent   carbohydrate   of

38.7   - 56.3 and 9.4 - 10.7 respectively,   whereas   wheat

germ   agglutinin,   the   nonglycoprotein   gives   negative

results.

3.5.6   Stability   of rice   lectin.   Purified   rice

lectin   whether   from   bran,   root   or   embryo   is   quite

stable.   The   specific activity of rice   lectin   remains

100% of the initial activity after incubation in PBS   pH

7.4 at various temperatures 0-70 ^{O}C for 2 h, beyond this

point, the specific activity rapidly decreases to 50% at

80°C   and   is   completely   lost   at   100°C   (Fig.   21A).

Exposure   of   lectin at various pH(1-13) for 24   h,   and

then   dialyzed against PBS pH 7.4 demonstrate   stability

of   rice   lectin   between pH 2 to 12   as   seen   by   100%

recovery   of   specific activity of the   dialyzed   lectin

(Fig. 21B).

Table 11 The amount of carbohydrate in rice lectin.

Rice lectin	% (w/w) total carbohydrate in lectin	
	by using D-Glc as standard	by using L-Ara as standard
Bran lectin	7.5	0.9
Embryo lectin	2.8	4.5
Root lectin	8.1	9.1

Figure 21 Percentage of specific hemagglutinating activity after treatment rice lectin in various temperature (A) and hydrogen ion concentration (B).
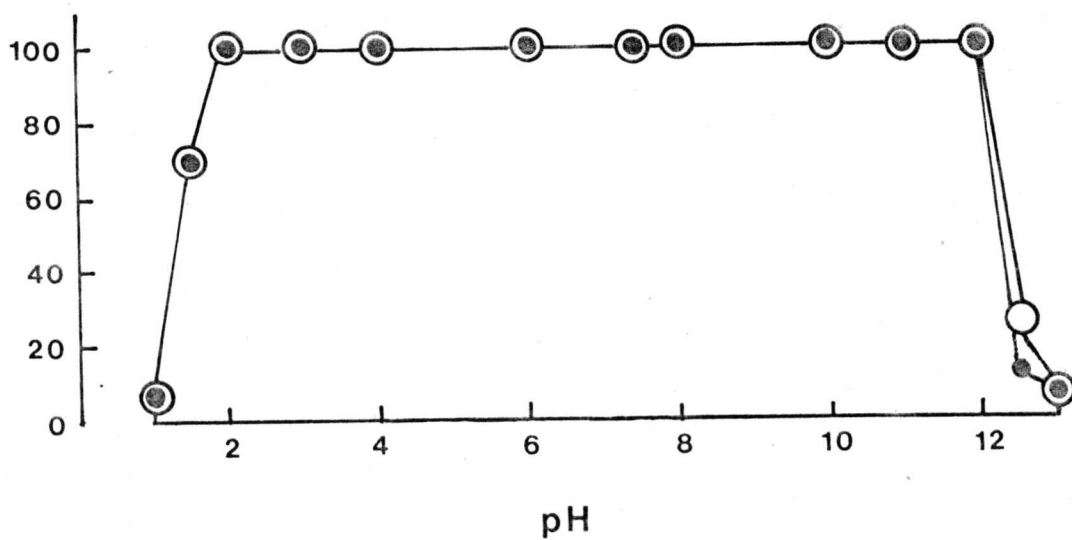
In A.(o——o)represents for either bran lectin or embryo lectin or root lectin and in B.(●——●) represents for either embryo lectin or root lectin and (o——o) for bran lectin.

A.

% specific activity

Temperature (°C)
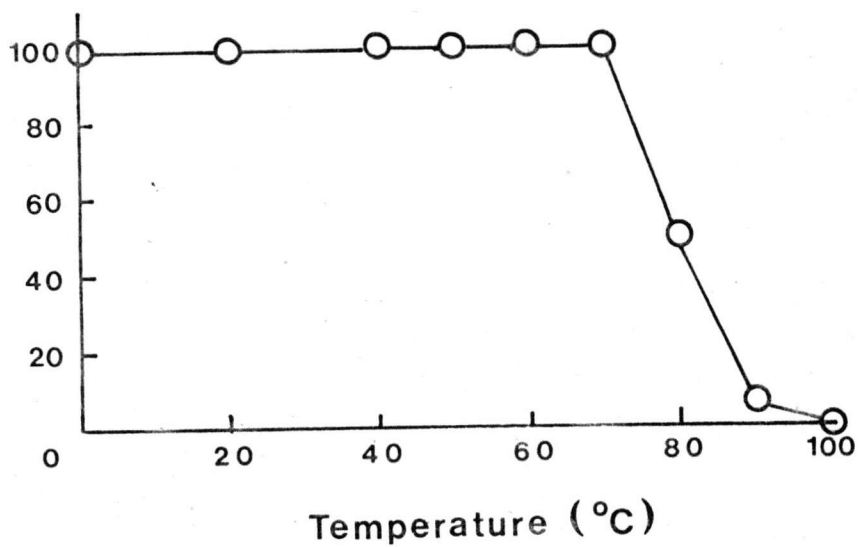
B.

% specific activity

pH

3.6 Bacterial agglutination by rice lectin.

Purified rice lectin (20 μg/60 ul) from bran or embryo or root similarly aggluginate R15 and R17 (2×10^6 cells). Agglutination was negligible without lectin and in the presence of both lectin and GlcNAc (20μg/60μl), whereas non-associative *E. coli* forms no agglutination in all case (Fig. 22).

3.7 Binding of rice embryo lectin to R15 and R17.

The ^{14}C-labelling of EL with acetic anhydride did not destroy the lectin activity. Binding of ^{14}C-embryo lectin to N_2-fixing bacteria assayed by graphical analysis of Scatchard plot shows a modest degree of nonlinearity in both R15 and R17 (Fig 23). This phenomenon could be due to the negative cooperativity of multiple lectin binding sites and/or the presence of heterogeneous lectin receptors. Further analysis was performed by different models of cooperativity; 1) Statistical Mechanical Model, 2) Two-step Adair Model and 3) De Meyts' Model, which resulted in various binding parameters as shown in Table 12. The binding affinity of rice lectin to R15 and R17 calculated by any models are in the same range of 1.02-8.82 and 0.58-4.80

Figure 22   Bacterial agglutination by rice lectin.

A   R15 and rice embryo lectin.

B   R17 and rice embryo lectin.
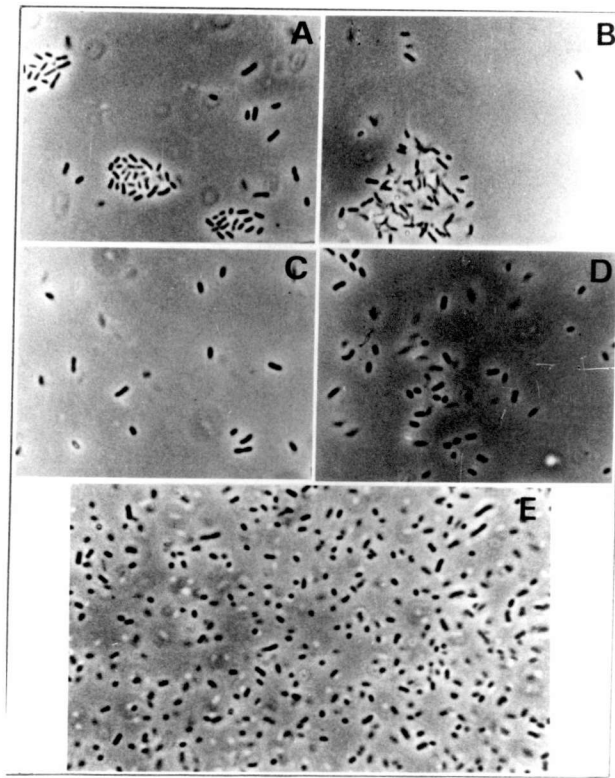
C   Agglutination   of   R15   by   rice   embryo

        lectin is inhibited by GlcNAc.

D   Agglutination   of   R17   by   rice   embryo

        lectin is inhibited by GlcNAc.

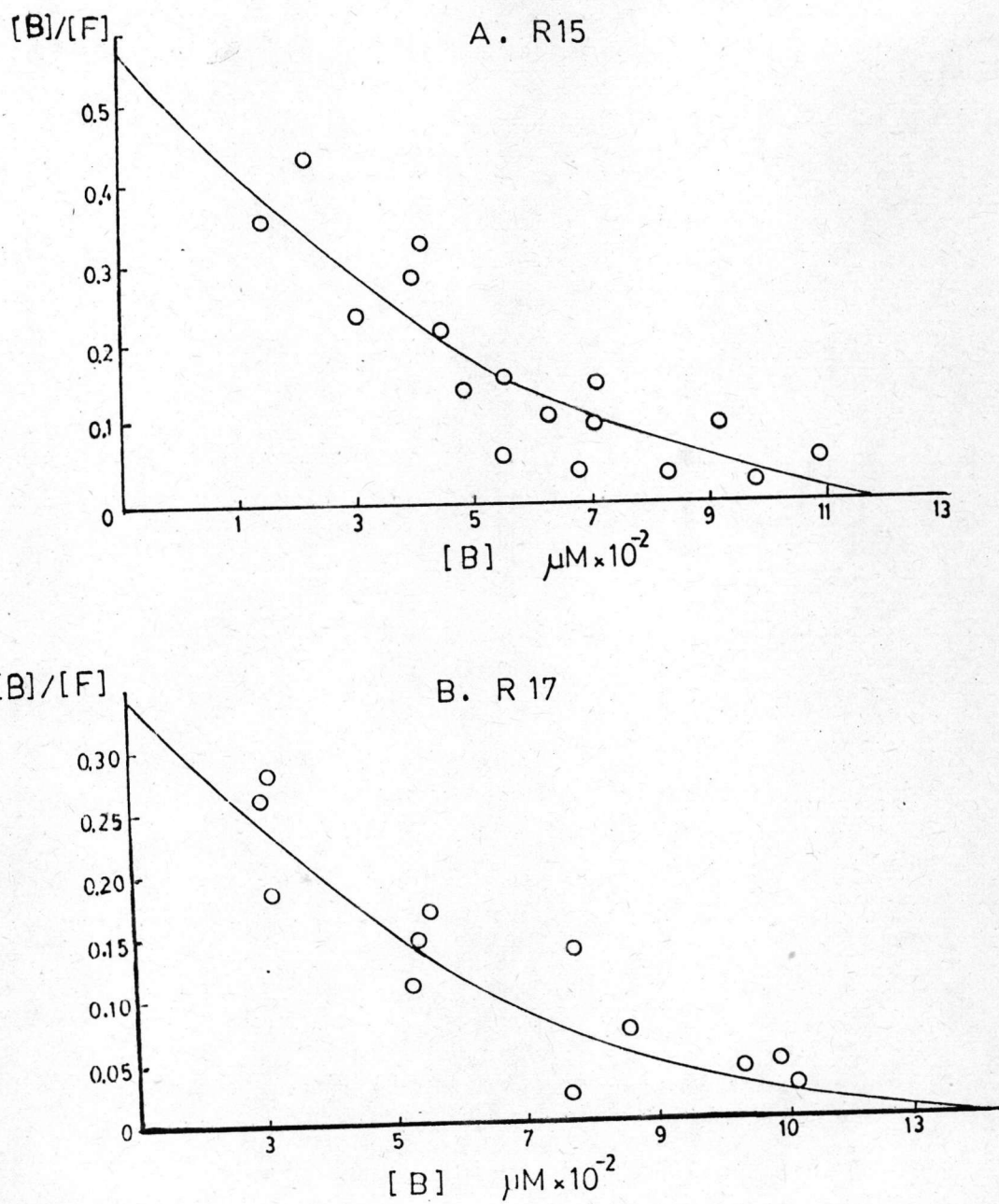E   *E.   coli*   K12   and   rice   embryo   lectin.

        (Magnification 1000 x)

Figure 23 Scatchard plot of specific binding of ^{14}C-EL

to *Klebsiella R15* (A) and *Klebsiella* R17 (B).

Table 12 Characterization of lectin binding sites on R15 and R17 by
different models of cooperativity.

Model of Cooperativity	Binding parameters		Lectin binding site on	
			R15	R17
Statistical	K μM^{-1}		4.41	2.40
Mechanical	R_0 μM		0.13	0.14
Model	$\mu mol.cell^{-1}$		1.3×10^{-12}	1.4×10^{-12}
	β		0.53	0.25
Two-step				
Adair Model	K_1 μM^{-1}		8.82	4.80
	K_2 μM^{-1}		1.02	0.58
	P_0 μM		0.06	0.07
	$\mu mol.cell^{-1}$		0.6×10^{-12}	0.7×10^{-12}
De Meyts'	K μM^{-1}		4.41	2.40
Model	R_0 μM		0.13	0.14
	$\mu mol.cell^{-1}$		1.3×10^{-12}	1.4×10^{-12}
	δ		2.16	2.07

R_0 = concentration of [Total] lectin binding sites.

β = Cooperativity parameter

δ = Parameter specifying occupancy dependency of affinity
(cooperativity parameter) in the occupancy-dependent affinity
model

P_0 = Concentration of heterogeneous lectin binding sites

K_j = Affinity of the jth subclass of lectin binding site

μM^{-1} respectively, which indicate higher affinity of lectin binding to R17. The cooperativity parameters, β of both R15 and R17 were <1, and δ>1 which show negative cooperativity of multiple lectin binding sites. Although the heterogeneity of lectin receptors could not be proved by these results, but the total concentration of lectin receptors on R15 and R17 were shown to be very similar (1.3×10^{-12} and 1.4×10^{-12} $\mu mol.cell^{-1}$).

3.8   Competitive binding assay of embryo lectin receptor.

Since the previous results (3.6) indicate that rice lectin purified from embryo, root and bran show the same effect on the agglutination of R15 and R17, in this experiment, root lectin, GlcNAc and cold embryo lectin were used as competitors to compete with ^{14}C-EL for the lectin receptors on bacterial cells.

Fig. 24 shows similar competitive potential of RL comparing to cold EL which means that either RL or EL should occupy the same receptor on the bacterial surface. GlcNAc inhibits binding of embryo lectin on both R15 and R17, implying that sugar specificity is required for lectin-bacterium binding.

Figure 24 Competitive binding assay using EL, RL, and GlcNAc as competitors.

A. and B. are the binding of ^{14}C-EL to *Klebsiella* R15 and R17 respectively; (●——●) total binding without competitor, (○——○) in the presence of 100x cold EL, (△——△) in the presence of 100x cold RL, and (▲——▲) in the presence of 0.9 M GlcNAc.

[B]
μM×10⁻²

A. R15

¹⁴C EL (10⁻² μM)

[B]
μM×10⁻²

B. R17

¹⁴C EL (10⁻² ×μM)
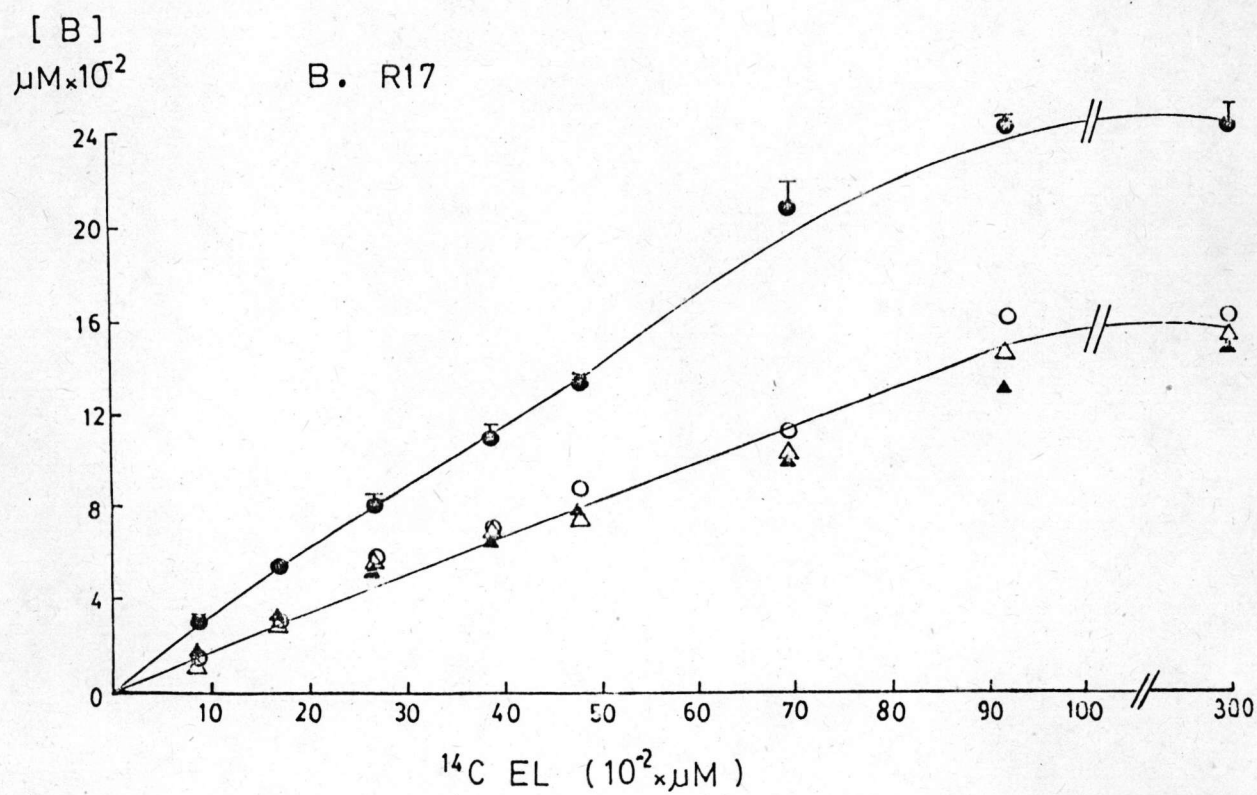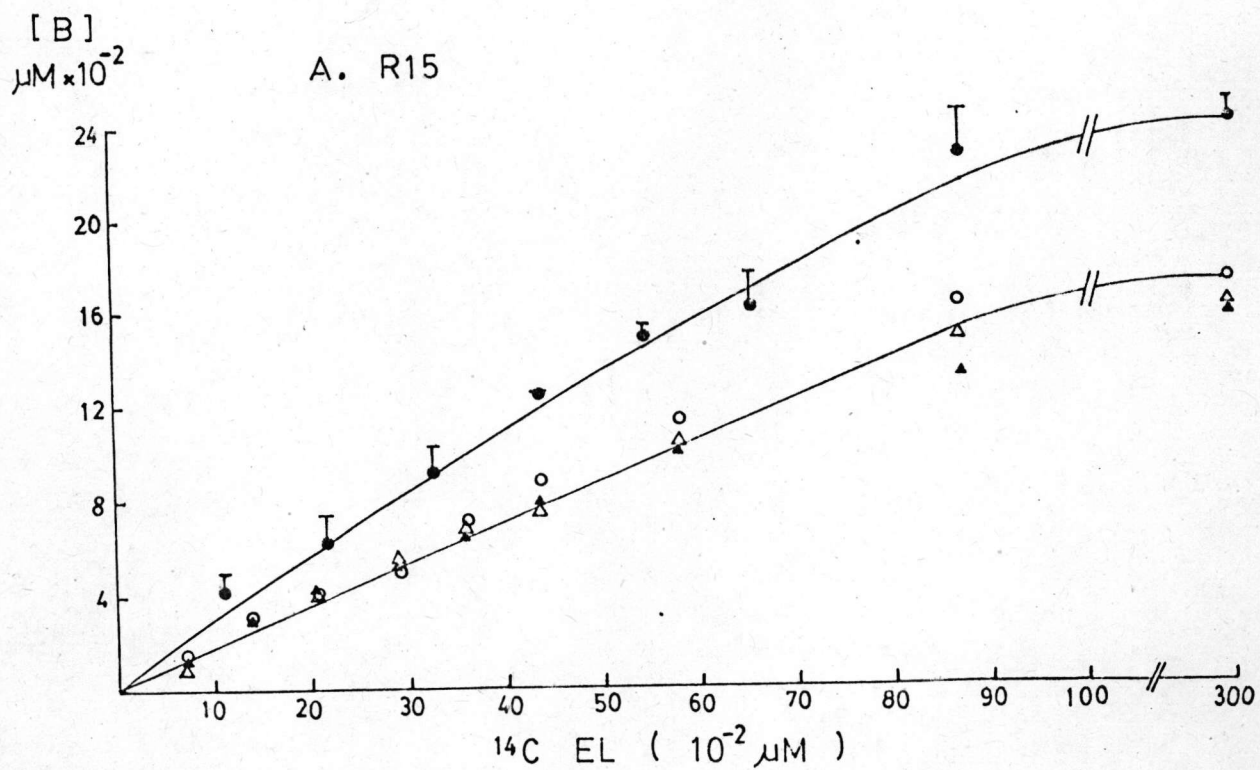
3.9   Enhancement of bacterial attachment by addition of

root exudate or lectin.

From   the   previous   results   (3.1.1),   attachment

of   R15   and   R17   to   rice   (cv.RD7)   root   epidermis   were

observed after 2 h and micronodules were formed at 36   h

after   inoculation.   In this experiment, the   effect   of

root   exudate containing rice lectin or purified   lectin

on   bacteria-plant   attachment   was   tested.   The   PBS-

washed   excis d roots from 7-day-old rice seedlings   and

acridine   orange-labelled   bacteria   were   prepared   as

described in 2.14. Bacterial attachment on root   surface

was observed under epi-fluorescence microscope at 2   and

36 h after bacterial inoculation.   The addition of   root

exudate   or purified lectin enhanced attachment   of   R15

and   R17 to the PBS-washed excised root (Table 13).   In

control tubes, using PBS as affector and *E. coli* instead

of   nitrogen-fixing bacteria, negligible attachment (NA)

was   observed.   Addition of GlcNAc, the   specific   sugar

inhibitor   of   lectin can overcome enhancement   by   both

root exudate and lectin.

Table 13 Effect of rice lectin on the attachment of R15 and R17 to
PBS-washed excised roots rice (cv. RD7).

The PBS-wasked excised roots from 3 seedlings (7-day-old) in 5 ml PBS
were inoculated with acridine orange labelled bacteria in the presence
of 4 mg dry matter of root exudate or 1 µg purified lectin, then bacterial
attachment was viewed under epi-fluorecence microscope after 2 and 36 h.
Duplicate sample in each treatment were done. For control either GlcNAc
was added 44.2 mg or no effector in the incubation medium.

Effectors (amount)	Bacterial inculum	Bacterial attachment	
		2 h after inoculation	36 h after inoculation
	(2 x 10^8 cells)		
PBS	R15	NA	NA
	R17	NA	NA
	E.coli	NA	NA
root exudate	R15	loose clusters	numerous micronodules
(4 mg dry matter)	R17	loose clusters	numerous micronodules
	E.coli	NA	NA
root exudate + GlcNAc	R15	NA	NA
(4 mg dry matter)(44.2 mg)	R17	NA	NA
	E.coli	NA	NA
RL	R15	loose clusters	numerous micronodules
(1 µg)	R17	loose clusters	numerous micronodules
	E. coli	NA	NA
EL	R15	loose clusters	numerous micronodules
(1 µg)	R17	loose clusters	numrous micronodules
	E. coli	NA	NA
BL	R15	loose clusters	numerous micronodules
(1 µg)	R17	loose clusters	numerous micronodules
	E. coli	NA	NA
RL or EL or BL + GlcNAc	R15	NA	NA
(1 µg) (44.2 mg)	R17	NA	NA
	E. coli	NA	NA

NA = Negligible attachment

3.10 Localization of lectin receptor by colloidal gold technique.

To localize lectin receptors, gold is used as marker because of its high electron density and its ability to conjugate to protein being studied, so that the protein-gold complex can be traced specifically under electron microscope.

3.10.1 Preparation of colloidal gold. Monodisperse gold sols were prepared to be 5 nm (Au_5) and 12 nm (Au_{12}) in diameter from gold chloride by varying the reducing agent both qualitatively and quantitatively as described in Methods 2.36.1. The average particles size of prepared colloidal gold sols were determined by measuring the diameter of 100 particles viewed in electron microscope. Gold granules selected for use in localization of lectin receptor in further experiment were constantly round shape (with eccentricity ~1) and uniform in size (Table 14).

3.10.2 Preparation of protein-gold marker. Lectin receptor can be localized by direct and indirect method. For direct method, complex of RL-Au is used to localize lectin receptor, whereas for indirect method, lectin

Table 14   Physical data of prepared gold colloids.

Particle diameter[a] (nm ± SD)	Eccentricity[b]	pH[c]	Color	Absorption, λmax (nm)
5.2 ± 1.1	1.0	7.4	red	518
12.3 ± 4.0	1.0	7.9	orange-red	523

a. average of 100 particles counted on electron micrograph;

   SD = standard deviation

b. ratio of larger to smaller axis of the same particle

c. measured after addition of 0.05 ml 1% PEG 20,000 per ml of colloid.

site with RL which in turn is detected with gold granules conjugated with ovomucoid(OV-Au). Thus, RL-Au and OV-Au were prepared and used as markers. Two criteria were considered in preparing RL-Au and OV-Au, i) optimization of protein-gold conjugation, and ii) validity of this complex.

3.10.2.1 Optimization of protein-gold conjugation. Colloidal gold is a negatively-charged hydrophobic sol where stability is maintained by electrostatic repulsion. The addition of electrolytes results in the compression of the ionic double layers and in the reduction of the radius of action of repulsive forces. As a result gold sols will flocculate. Flocculation of gold granules can be prevented by adding a protective protein coat on the particles by mixing a gold sol with a soluble protein. Adsorption of proteins to colloidal gold depends on the concentration of protein and its pI.

a) Optimum amount of protein to stabilize colloidal gold. The optimal amount of protein necessary to stabilize a gold sol was determined by exposing constant amounts of gold to various concentrations of protein, then the unstabilized gold granules was flocculated by adding 1% NaCl. Flocculation was

observed by a colour change of gold sol from red to light blue which is determined by the decreasing of A_{520}. Fig. 25 shows that the optimal concentration of RL to stabilize colloidal gold Au_5 and Au_{12} (A_{520} = 1.4) are 12.5 and 25 $\mu g.ml^{-1}$ respectively, whereas the optimal concentration of OV are 6.25 and 50 $\mu g.ml^{-1}$ respectively.

b) Optimum pH of protein-colloidal gold conjugation. The optimum pH for adsorption of RL and OV on colloidal gold were determined to be 3-6.5 and 4-5 respectively (Fig. 26). The pH adsorption isotherm differs in 3 regions, i) at acidic pH lower than the pI of protein (pI for OV = 3.9-4.3, RL = 4.5-5.1), ii) at those pH close to the pI, and iii) at the pH above the pI. The pH range most probable for stabilizing colloidal gold resulted in maximum adsorption lies around pI.

3.10.2.2 Validity of protein-gold complex. Well stabilized RL-Au and OV-Au complexes, prepared under all the optimal conditions tested, conjugate with chitin pellet and wheat germ pellet by showing dark red color. Storage of these protein-gold complexes at 4 ^oC stabilizes their validity for several months.
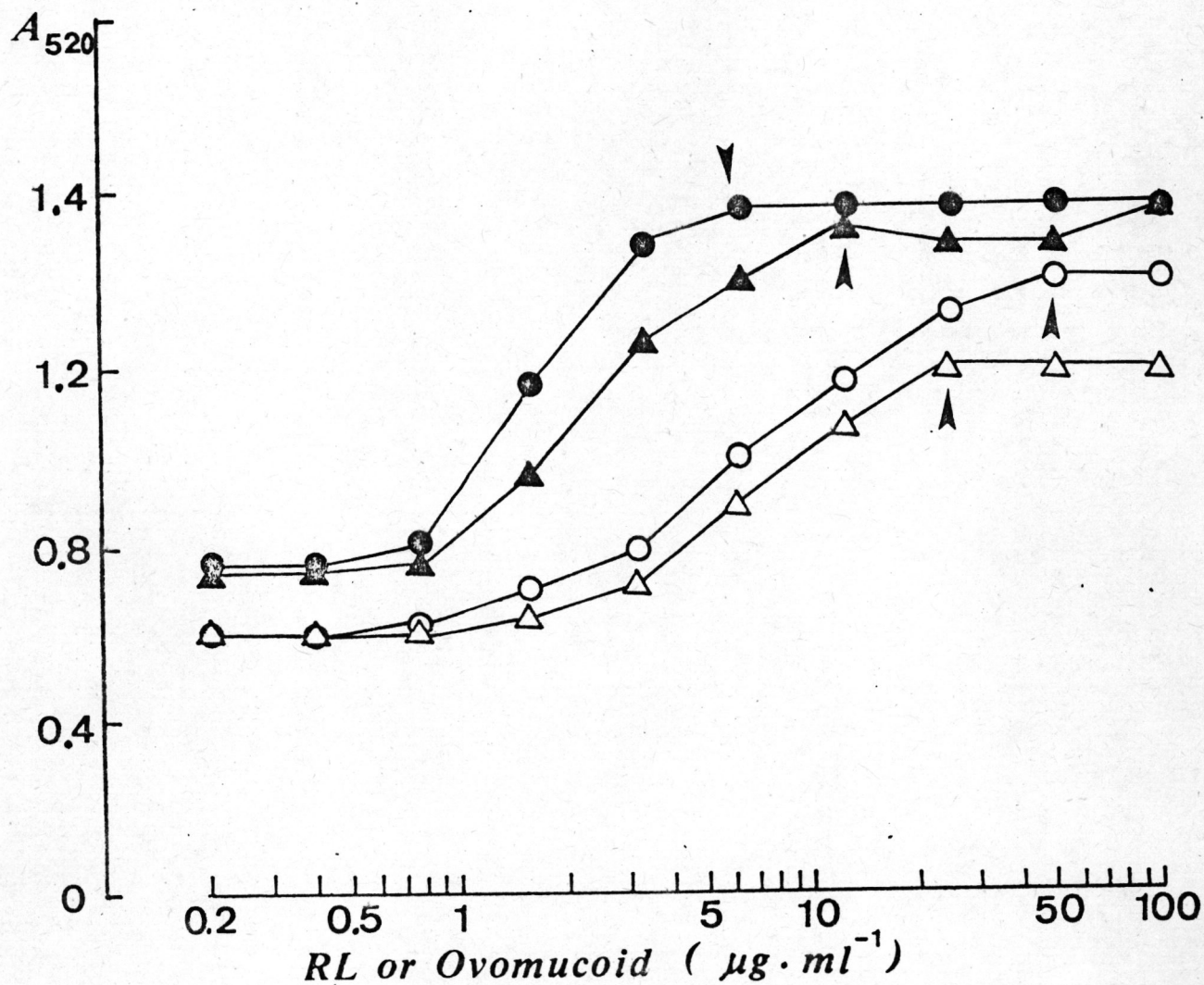
Figure 25 Adsorption isotherm of rice root lectin and ovomucoid on colloidal gold, (●————●)OV-Au$_5$, (○————○)OV-Au$_{12}$, (▲————▲)RL-Au$_5$, (△————△)RL-Au$_{12}$. A decrease in absorbancy indicated a decrease in the stabilization of colloidal gold. The arrows correspond to the amount of RL or ovomucoid sufficient to fully stabilize the colloids.
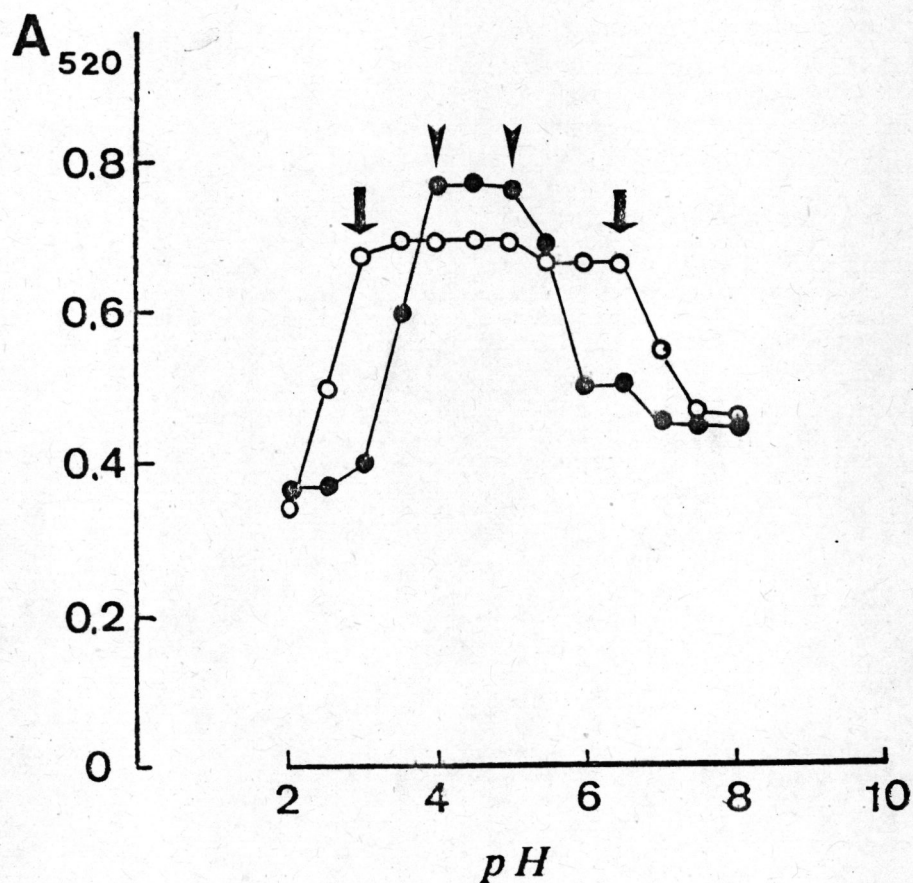
Figure 26   The pH adsorption isotherm of rice root

lectin and ovomucoid on colloidal gold,(●——●) OV-Au$_5$ and

(○——○)RL-Au$_5$.   A decrease in absorbancy indicated a

decrease in the stabilization of colloidal gold.   The

arrows correspond to the optimum pH range for OV-Au and

RL-Au which are pH 4-5 and 3-6.5 respectively.

3.11 Localization of bacterial lectin receptor.

Since free living R15 and R17 fix nitrogen only in NF medium, it is interesting to compare the presence of lectin receptor on bacterial surface both in nitrogen-free (NF) and nitrogen-rich (RM) conditions.

Ultrastructure of R15 cultivated in RM shows the presence of glycocalyx or polysaccharide containing component outside the cell wall (Fig. 27A-B and 28A-C), which is not observed in R17 (Fig. 27C-D and 28D-F). In NF condition, glycocalyx is produced in both R15 and R17 (Fig. 29 - 30) at higher amount comparing to cultivation in RM. Many cells of R15 and R17 cultivated in NF demonstrate polar capsular polysaccharide outside the cell wall, and regions of low electron density inside the cells (Fig. 29A-C and 30D-E).

Bacterial lectin receptor can be localized by both direct and indirect gold labelling techniques. Although the indirect method has the advantage that RL upon binding to the cell receptor can protrude more freely and providing greater stereochemical accessibility of $OV-Au_5$ comparing to the direct method with $RL-Au_{12}$ complex, no significant different is observed among the two methods.

In control experiments for i) direct labelling, in which GlcNAc was coincubated with RL-Au during conjugation with either R15 or R17, negligible amount of gold particle is observed (Fig. 27A,C and 29A,C); and ii) indirect labelling, very few gold particles are observed in either incubation of R15 and R17 in the presence of RL and GlcNAc (Fig. 28A,D and 30A,D) or using of self conjugated OV-Au$_5$ omitting RL (Fig. 28B,E and 30B,E).

For strain R15, gold labelled lectin receptors cultivated in RM appear to be on the glycocalyx (Fig. 27B and 28C) and only some are on the cell wall as shown by indirect labelling (Fig.28C), whereas for strain R17 cultivated in RM, without the production of glycocalyx, lectin receptors are clearly attached on the cell wall (Fig. 27D and 28F).

Distribution of lectin receptors on R15 and R17 cultivated in NF medium are on both glycocalyx and cell wall (Fig. 29D and 30F). It is noted that glycocalyx produced by R17 in NF condition appears to be much more than by R15 (Fig. 29-30) and therefore, gold labelled lectin receptors localized in the vicinity of R17 should be more than that of R15.

<u>**Figure 27**</u> Ultrastructural localization of gold-labelled

lectin receptors on the surface of bacteria R15 and R17

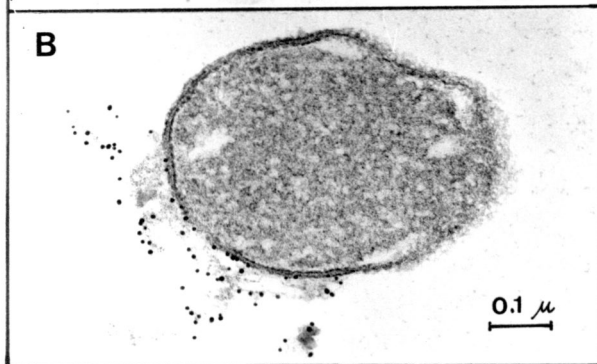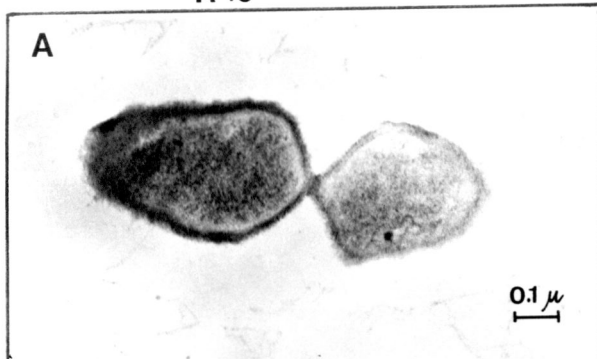cultivated in rich medium (RM) by direct labelling.

A, C   Control, in the presence of GlcNAc.

B $RL-Au_5$-labelled   lectin   receptors   are

            localized on the cell wall of R15.

D $RL-Au_{12}$-labelled   lectin   receptor   are

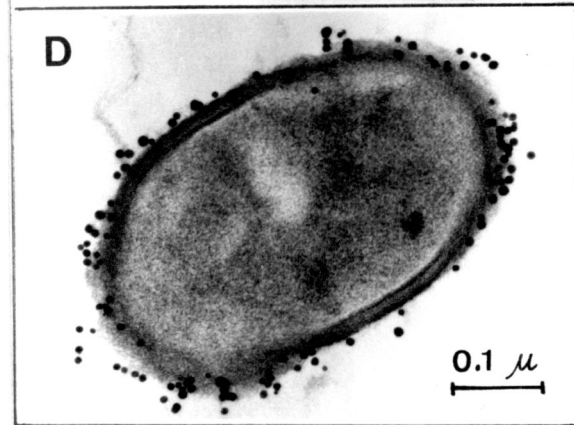   localized on the cell wall of R17.

R 15   *RM*

A

0.1 μ
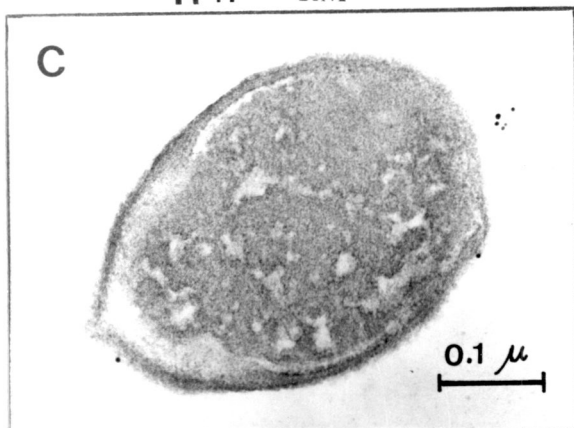
B

0.1 μ

R 17   *RM*

C

0.1 μ

D

0.1 μ

Figure 28   Ultrastructural localization of gold labelled

lectin receptors on the surface of bacterial R15 and R17

cultivated in RM by indirect labelling with OV-Au$_5$.

A, D   Control, in the presence of GlcNAc.

B, E   Control, bacteria were directly incubated

              with OV-Au$_5$. Very few gold granules are

              observed.

C   OV-Au$_5$ conjugated lectin receptors are

              localized on capsular material and cell wall

              of R15.

F   Lectin receptors labelled by OV-Au$_5$ are shown

              on cell wall of R17.

R 15   *RM*

A   B

0.1 μ   0.1 μ

C

0.1μ
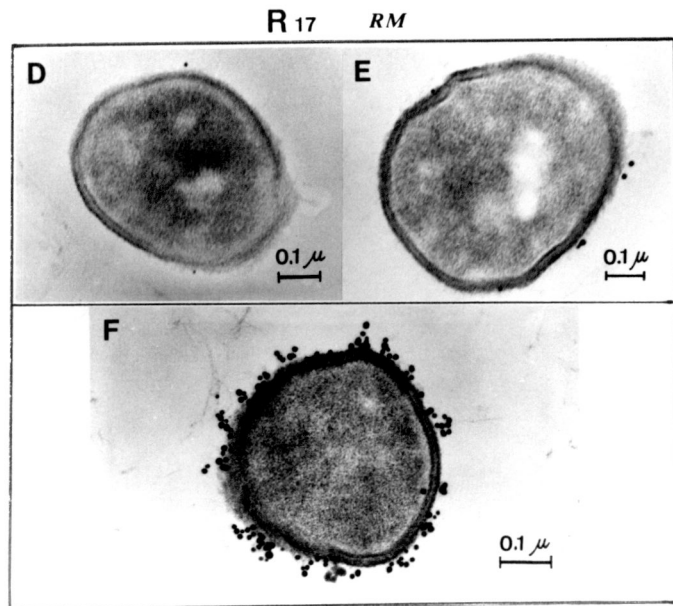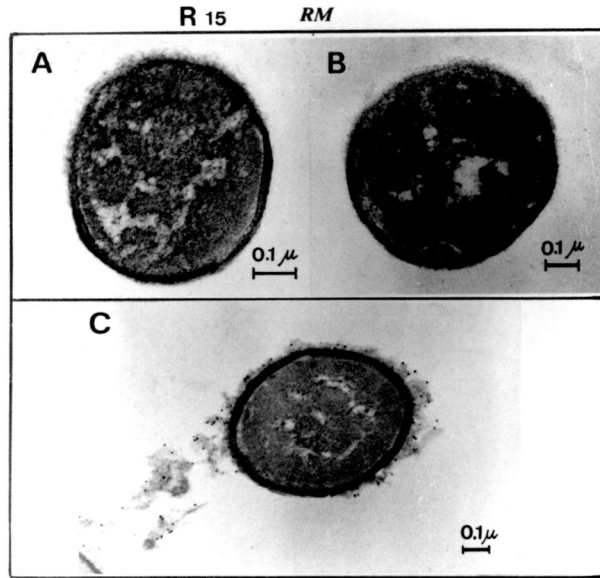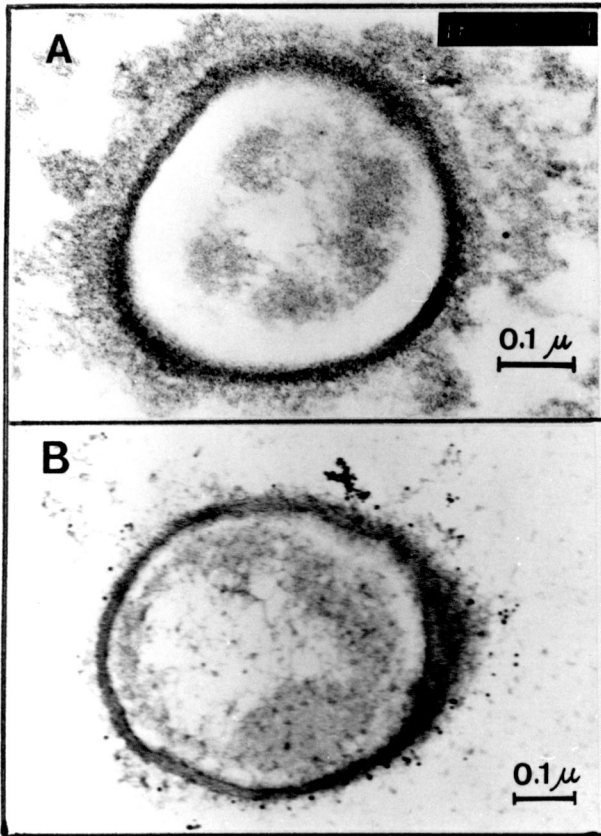
R 17   *RM*

D   E

0.1 μ   0.1 μ

F

0.1 μ

Figure 29 Ultrastructural localization of gold labelled lectin receptors on the surface of bacteria R15 and R17 cultivated in NF medium by direct labelling with RL-Au$_5$.

A, C   Control, in the presence of GlcNAc.

B, D   Gold-labelled lectin receptors are localized on capsular material and cell wall of R15 and R17.

R 15 *NF*

A

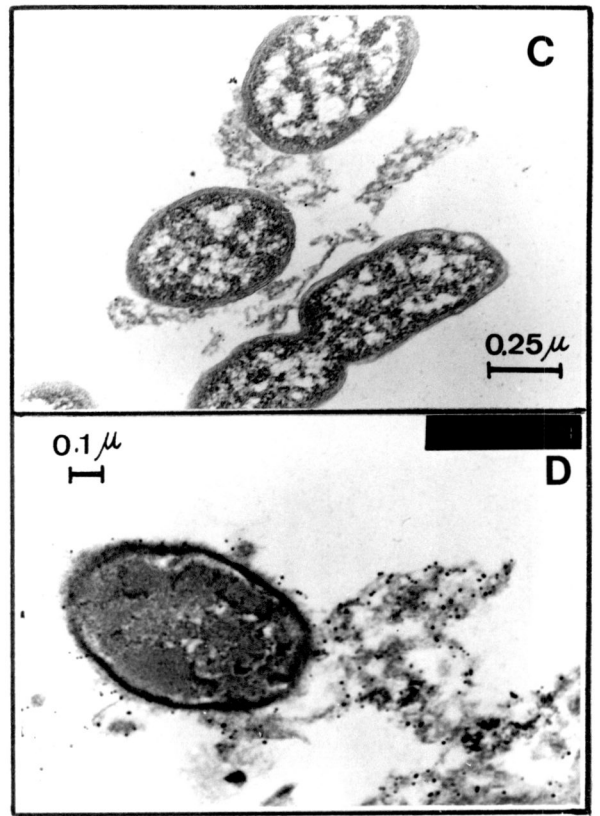0.1 μ

B

0.1 μ

R 17 *NF*

C

0.25 μ

0.1 μ

D

<u>Figure 30</u> Ultrastructural localization of gold labelled
lectin receptors on the surface of bacteria R15 and R17
cultivated in NF medium indirect labelling with OV-Au$_5$.

A, D   Control, in the presence of GlcNAc.

B, E   Control, bacteria were directly incubated
            with OV-Au$_5$.   Very few gold granules are
            observed.

C, F   Lectin receptors are localized on capsular
            material and cell wall of R15 and R17.

R 15 *NF*

A

0.1 μ

B

0.2 μ

C

0.1 μ

R 17 *NF*

D

0.1 μ

E

0.1 μ

F

0.1 μ
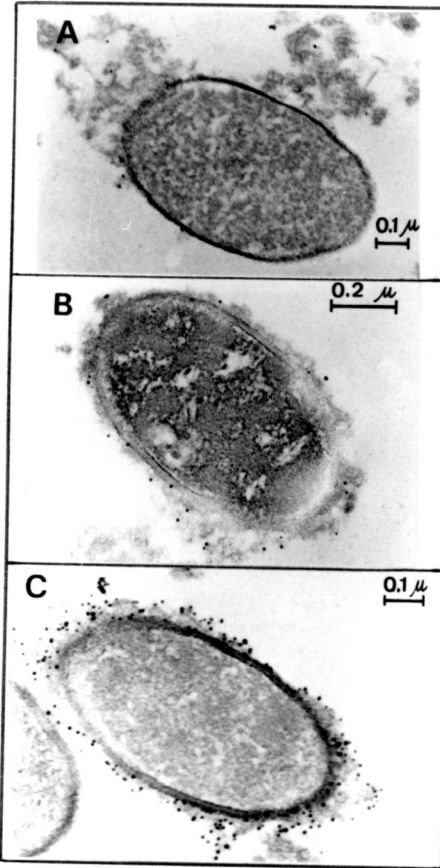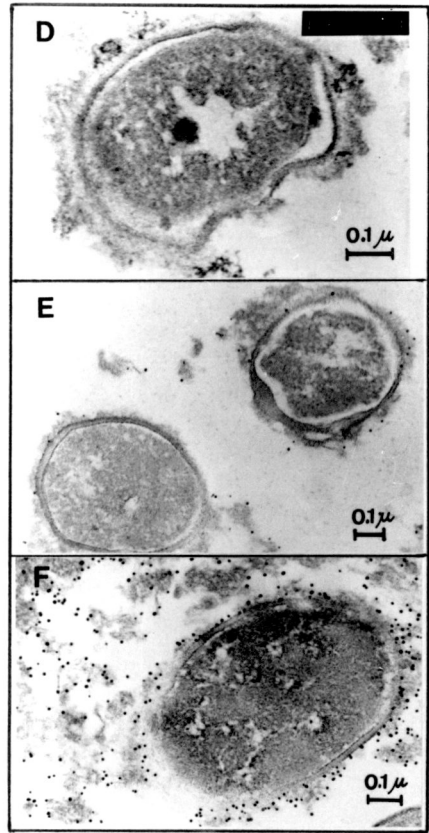
These results indicate the potential of root lectin excreted by rice seedling as the associative factor to recognize and agglutinate N_2-fixing R15 and R17 no matter in N-sufficient or N-deficient environment. However in NF condition with increased production of glycocalyx, where lectin receptors reside, association between plant and bacteria mediated by lectin should be enhanced.

3.12 Localization of lectin receptor on rice epidermis.

Control rice seedling roots, incubated with RL-Au$_5$ in the presence of GlcNAc for direct labelling, do not conjugate with any gold particles whether the roots were pre-fixed in glutaraldehyde before conjugation or not (Fig. 31A-B and 32A-B).

For direct labelling of lectin receptors without GlcNAc, RL-Au$_5$ significantly binds to both glutaraldehyde fixed roots (Fig. 31C-F) and unfixed roots (Fig. 32C-F). These gold-labelled lectin receptors were observed all over the outer periphery of epidermal cells, and especially more concentrated on the

muci gel, or polysaccharide excretory substances outside epidermal cells.

Control root samples for indirect labelling, in which GlcNAc was added together with RL prior to incubation with roots, no gold particles are shown in Fig. 33A and 34A, as well as the other control experiment which only OV-Au$_5$ was added without RL, the base-line conjugation of OV-Au$_5$ *per se* on rice epidermal cells was minimal (Fig. 33C-D and 34C-D).

For indirect labelling of lectin receptor by OV-Au$_5$, in which roots (fixed with glutaraldehyde and unfixed) were preincubated with RL, and then localized these bound lectin by conjugation with OV-Au$_5$, gold labelled lectin receptors were clearly demonstrated on the outer periphery of root epidermis (Fig. 33E-H and 34 E-H), especially on the extracellular components of high and medium electron density.

Figure 31   Ultrastructural localization of gold labelled

lectin receptors on glutaraldehyde-fixed root epidermis

by direct labelling with RL-Au$_5$.

A - B   Control, in the presence of GlcNAc.

C - F   Gold-labelled lectin receptors are localized

               along the outer surface of root epidermis.

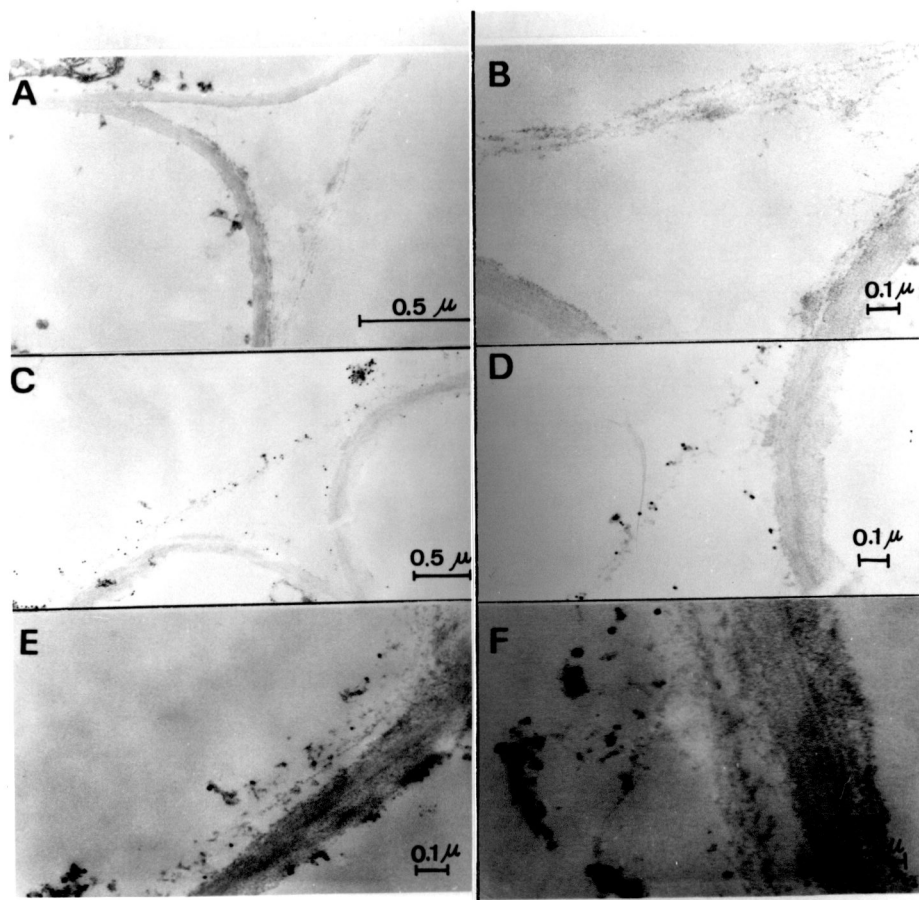   Note the gold labelling in the extracellular

               slime.

Figure 32   Ultrastructural localization of gold labelled lectin receptors on root epidermis of rice (cv. RD7) by direct labelling with RL-Au$_5$.

A - B   Control, in the presence of GlcNAc.

C - F   Gold-labelled lectin receptors are localized along the outer surface of root epidermis. Note the gold labelling in extracellular component.
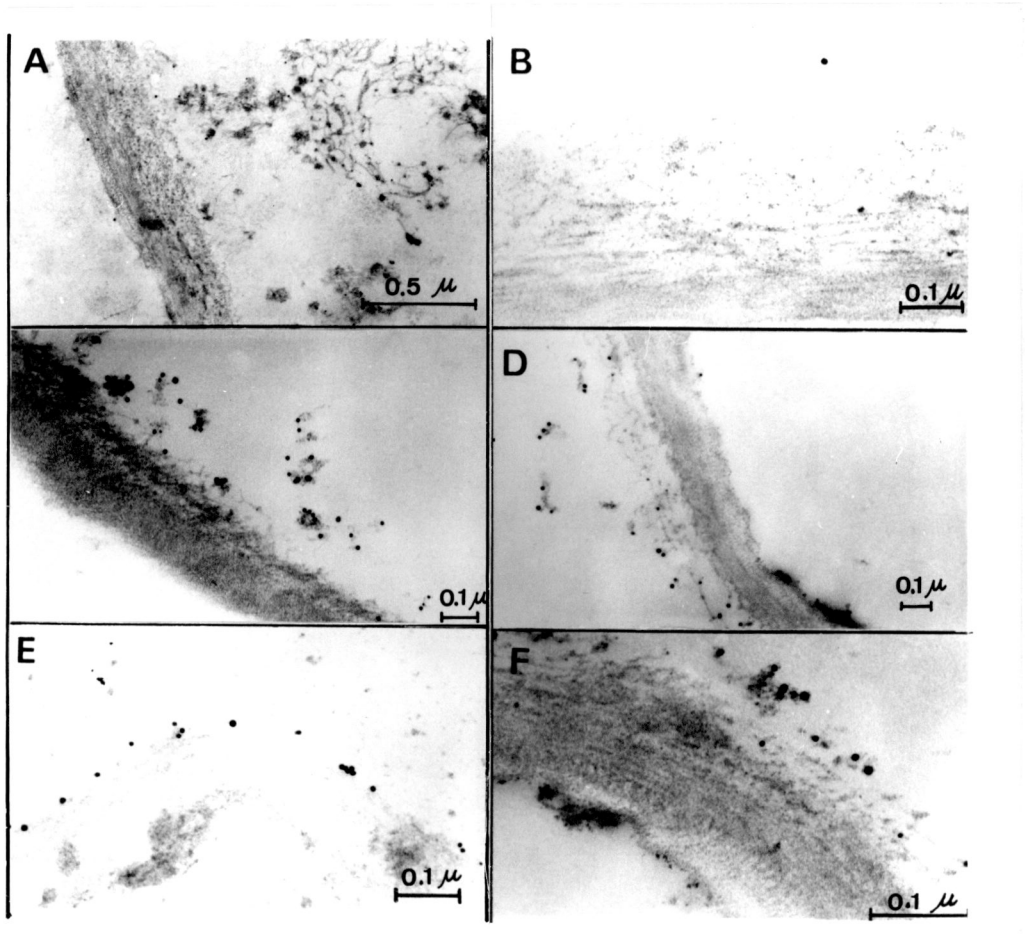
A — 0.5 μ
B — 0.1 μ
— 0.1 μ
D — 0.1 μ
E — 0.1 μ
F — 0.1 μ

Figure 33 Ultrastructural localization of gold labelled lectin receptors on glutaraldehyde-fixed root epidermis by indirect labelling with OV-Au$_5$.

A - B   Control, root was incubated with RL and GlcNAc prior to OV-Au$_5$.

C - D   Control, root was directly incubated with OV-Au$_5$. Very few gold granules are observed.

E - H   Gold particles are cleary demonstrated on the root epidermis when root was incubated in RL prior to labelling with OV-Au$_5$. Note the presence of gold granules with extracellular slime.
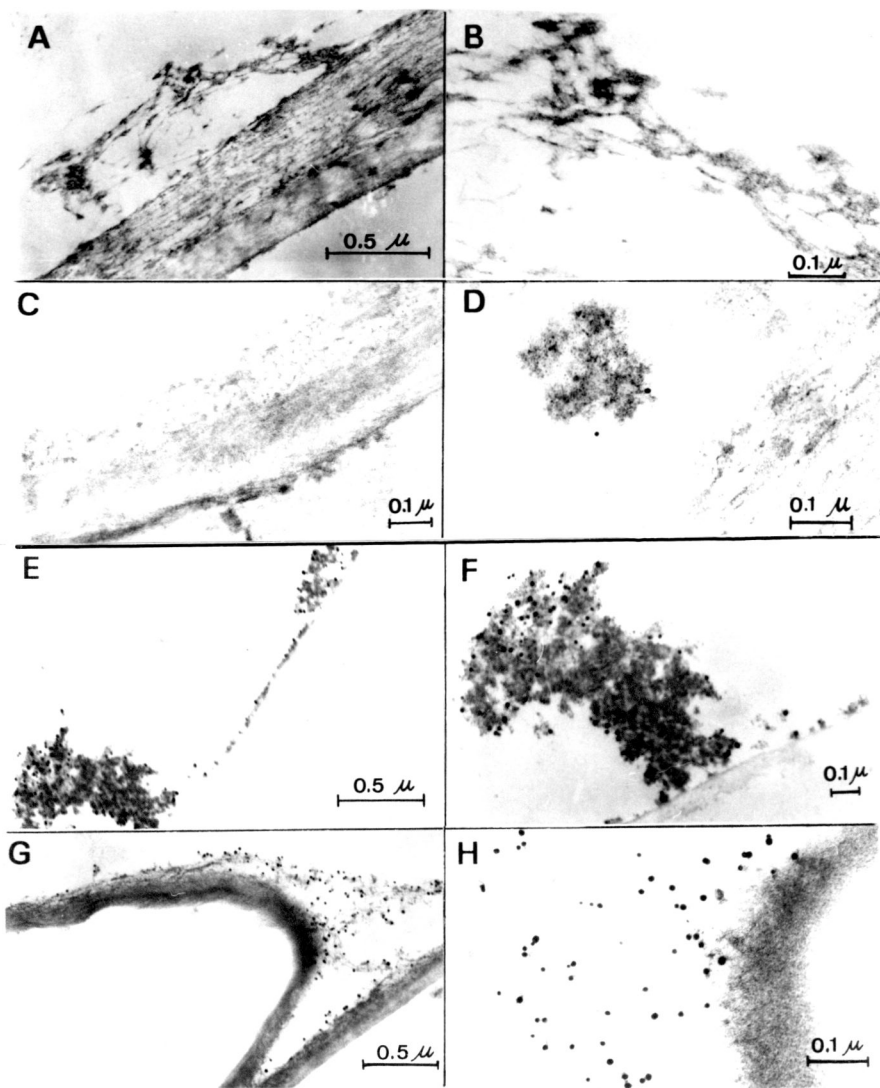
Figure 34 Ultrastructural localizatin of gold-labelled

lectin receptors on root epidermis by indirect labelling

with OV-Au$_5$.

A - B   Control, root   was   incubated with RL and

            GlcNAc prior to OV-Au$_5$.

C - D   Control, root was directly incubated with OV-

            Au$_5$. Very few gold granules are observed.

E - H   Gold   particles are clearly demonstrated on

            the root epidermis when root was incubated in

            RL prior to labelling with OV-Au$_5$.